PROJECT DESCRIPTION SHEET

Name of the candidate: Ingrid Swensen

Thesis title (Norwegian):

Thesis title (English):   Modeling and non-linear control of gel breaking in drilling operations

Background

As production on the Norwegian shelf enters tail production, many wells to be drilled require better control over the pressure in the well. This has motivated the use of automatic control systems for controlling downhole pressure, for example using automated Managed Pressure Drilling (MPD).

The fluid ("mud") used in drilling is on purpose non-Newtonian, and is "gelling". Gelling of drilling fluid is a severe non-linear phenomenon, which presents challenges for accurate pressure control. The task in this project work is to develop a nonlinear control structure that can improve pressure control under gelling.

Work description

1. Do a literature survey on fluids (muds) used in drilling, and describe the control problem.
2. Implement a simple model for the fluid part of a drilling system, with a fluid model that includes non-Newtonian features and gelling. The gelling part of the model could be inspired by mechanical friction models (keywords may be Coloumb, LuGre, etc.)
3. Implement a PID controller in a MPD control structure (pressure control by manipulating the choke), and simulate challenges that gelling gives in pressure control.
4. Suggest nonlinear control structures and algorithms that alleviate the problem (using choke opening/flow and pump flows as manipulated variables).

Start date: 6. January, 2014   **Due date:**   10. June, 2014

Supervisor: Lars Imsland
Co-advisor(s):   Espen Hauge and John-Morten Godhavn, Statoil

Trondheim, __10. January 2014_____

___ ⌇ ⌇ ⌇ ___

Lars Imsland
Supervisor

Abstract

As the petrolium operators are drilling deeper and more complicated well paths, extreme downhole presure variations during drilling operations may cause damage to equipment. This may in addition result in production restrictions and increased cost. Therefore, the main purpose of this project was to develop a non-linear control structure to stabilize the downhole pressure, such that the pressure never exceeds the $\pm$ 2 bar limit when the mud pump was started.

Mud pump startup is one of the main reasons for increased pressure. Mud at rest will, after some time, start the process of gelling. When the system is set to motion again, a considerable amount of force is therefore required to break the gel.

In order to achieve pressure stabilization, a controller was implemented on the mud pump. This controller included two proportional controllers, one monitored the downhole pressure, while the other used the calculated structure of the mud as an input parameter, meaning that the gelling was taken into account. The effects from a controlled back pressure pump were also assessed.

Incorporating automatic contol on the mud pump resulted in a downhole pressure that remained within the $\pm$ 2 bar boundaries. The pump was able to provide the desired flow rate in a reasonable amount of time. This is because the pump decreased the flow only when the downhole pressure increased at an excessive rate, giving the gelled mud more time to brake.

Throughout the project, the back pressure pump was implemented as a constant flow rate. A test scenario where the back pressure pump was a subject of automatic control showed a slight improvement with regards to downhole pressure stabilization, as well as a more stable choke valve opening. Automatic back pressure control might result in improved startup and shutdown timing.

With two controllers, one on the choke valve and one on the mud pump, a more stable mud break-down process can be achieved. This can lead to several economic advantages such as time saved when returning to reference flow rate, less wear on the choke valve, as well as fewer operators needed to handle the mud pump.

Sammendrag

Ettersom petroliumsindustrien borer dypere og mer kompliserte brønner kan store trykkvariasjoner under boreprosessen skape problemer, noe som kan føre til produksjonsbegrensninger og økte kostnader. Formålet med denne oppgaven er derfor å stabiliserer bunnhullstrykket ved å utvikle en ulineær kontrollstruktur, slik at trykket holder seg innenfor en begrensning på $\pm$ 2 bar når pumpen starter opp.

Oppstartsfasen for slampumpen er den mest kritiske perioden for trykkøkning i brønnen. Dette er fordi slam starter geledannelsen etter en viss tid, og når systemet igjen settes i gang, vil det kreve en betydelig kraft for å bryte opp slammet.

For å stabilisere trykket ble det implementert en regulator på slampumpen som pumper borevæske ut i systemet. Den består av to regulatorer, en som overvåker bunnhullstrykket og en som bruker et estimat av strukturen på borevæsken som inngangssignal. Det ble også forsøkt å sette på en regulator på baktrykkspumpuen.

Ved a bruke en regulert slampumpe er det mulig å få bunnhullstrykket til å holde seg innenfor $\pm$ 2 bar. Pumpen var i stand til å gi borevæsken den ønskede strømningshastigheten innenfor en rimelig tidsperiode, da strømningen kun ble begrenset dersom bunnhullstrykket steg for fort. Dette gav den geldannede borevæsken mer tid til nedbryting.

Baktrykkspumpen ble, gjennom mesteparten av prosjektet, implementert som en konstant strømning. Da en regulert baktrykkspumpe ble testet, viste en liten forbedring seg i stabiliteten til bunnhullstrykket, i tillegg til at ventilen viste seg å bli mer stabil. Ved å bruke en regulator var det også mulig å få bedre timing på oppstart og nedsteningen av pumpen.

Med to regulatorer, en på ventilen og en på slampumpen, var det mulig å skape en mer stabil nedbrytning av den geldannede borevæsken. Dette kan føre til flere økonomiske fordeler som spart tid når pumpen skal gi forventet strømningshastighet, mindre slitasje på ventilen i tillegg til at man kan spare inn på anntall arbeidere som kreves for å operere pumpen.

Acknowledgements

This master thesis was carried out from January 2014 to June 2014, the last semester of the 5th year of the MSc program in Engineering Cybernetics. All the work was conducted at NTNU.

The department of Cynernetics generously provided me with an office with a double screen computer and MATLAB® licenses, all of which have been indispenable in my completion of this project.

I would like to thank my supervisor at NTNU, professor Lars Imsland, for his helpful and always cogent and relevant guidance. I am also greatful to my co-advisor John-Morten Godhavn for suggesting that this subject would make a worthwhile project and for the quick respones when extra guidance was needed. In addition, a huge thanks should be directed to Robin Corcos, the teacher of the course "Writing for Science", who has corrected the language and grammar of the enire thesis.

Finally, I have to thank all of my fellow students, who consistently has been backing up and giving feedback on problems, often totally irrelevant for them.

Trondheim, June 2nd 2014

Ingrid Swensen

Contents

List of Figures

List of Tables

Listings

Figure 1: An illustration of the pump system.

1 | Introduction

1.1 Motivation

The control elements used on drilling rigs are of high importance. As the companies now are drilling deeper and more complicated well paths concerns inevitably arise about extreme pressures that are still uncontrolled. The inability to manage these kinds of downhole pressure might lead to production restrictions (MiSwaco; 2013) and increased costs

1.2 Managed Pressure Drilling

Managed Pressure Drilling is an adaptive process that makes it possible to control the pressure throughout the borewell. As can be seen from Figure 1, the system basically consist of a mud pump, a pipe, a drillbit, the well and a choke. All of these are hollow, such that a fluid can pass from the mud pump, downwards through the drillstring and thence out of the drillbit into the well.

The fluid used in well drilling is commonly known as 'mud'. This is a non-Newtonian fluid, or, in this project, a Bingham plastic, which will be described in greater detail in Section 2.2.1. The mud forms an annular flow from the drillbit and up to the head of the well where the Rotating Control Device (RCD) ensures that no fluid escapes through the surface, thus making this a *closed system*.

Because the system is closed, the pressure can be controlled by a choke, as shown in Figure 1. In order to improve pressure control, a back pressure pump

can be installed. This pumps mud back into the well and increases the downhole pressure (not modelled in this project).

When the mud has passed through the choke (described in Section 2.4.2), a container (the Mud Pit in Figure 1) rinses the mud and sends it back into the system.

1.3   The structure of the system

The system illustrated in Figure 1 is a simplified representation of a drill rig, consisting a pump, a drillstring and a choke valve. The pump provides mud from the mud container to the drillstring. The drillsting is a complex composoite device and has several functions, such as drilling, fluid trasportation, stabilizing and steering.

The system in this project consists of the following parts;

- Drillstring

  1. Pipe: transports the mud from the mud pump and adds torque to the drillbit.

  2. Bit: breaks up the rock in order for the well to become deeper. It also contains, among other things, a check valve (Sec. 2.4.3), which prevent the mud from going backwards.

- Well
- Choke valve
- Mud pump
- Back pressure pump

Other parts that may be interesting, but not included are;

- Collars: these form a part of the bottomhole assembly (BHA). They are heavy, thick-walled tubes that apply weight to the drillbit. As the well gets deepers, these are removed.
- Tools
- Heavyweight pipe

- BHA - may consist of several instruments as well as the bit. These can include

  - stabilizers
  - downhole motor
  - rotary steering
  - measurement while drilling
  - logging while drilling

1.3.1 Dynamics

There are several dynamics that may affect the flow, the following dynamics are included

- Rheology/Thixotropy of drilling fluid (gelling)
- Flow rate, q
- Laminar flow
- Dimensions (L_a, L_d, $d_{i,o,h-o}$)
- Pump and choke control

1.4 Thesis Outline

The structure of this project is shown to the left. **Chapter 1** is the Introduction and presents the different parts of the project.

Chapter 2 contains the background theory as well as the basic equations needed to understand the system. As can be seen on the left, there are two modelling chapters, which are intended to distinguish the standard MPD system from the extended MPD system.

The **first part of Chapter 3**, therefor, presents an MPD system used nowadays with a controlled choke valve and a back pressure pump, along with a model for the drilling fluid. An overview of model equations can be found in Table 3.1 on page 39. The **second part of Chapter 3** is the main focus of the project. This is where the mud pump is controlled. There is also added a further scenario, where both the mud pump and the back pressure pump are controlled. An overview can be found in Table 3.2 on page 3.2.

In the simulation chapter, **Chapter 4**, a brief overview of each of the modelled part of the system is presented, in order to clarify the workings of the controlled part.

Testing and final plots of the results are found in **Chapter 5**. For the readers convenience, the discussion around the plots are added in this chapter as well.

Finally, **Chapter 6** offers a conclusion, which includes suggestions for improvements and further work.

Everything that comes under the 'standard MPC system' is more or less taken from last year's project, Swensen (2013), with some additions and modifications.

2 | Theory

In this chapter the theory for each of the parts considered will be presented. Background information and general models needed to build the complete model are provided. Detailed derivation of the models is provided in the next chapter, Modelling.

2.1 The parts to be considered

A drilling device consists of a very substantial number of controllable components, which are considered in this project as forming three main parts of the system. The first part is the fluid used for drilling, the mud, along with its nonlinear properties. The second part deals with the pumps, which provide mud to the system. In the third part, the valves are examined, which choke the flow and which are primarily responsible for the main pressure control in the well. Because the mud has the properties of gelling, controllers need to be added to both the main pump and the check valve. Further, to enhance the reallity of the system, low pass filters are used to limit the rate of change of both choke and flow. A high pass filter is used as a differentiator for the downhole pressure.

2.2 The Drilling Mud

Because of gelling, the mud causes nonlinear pressure loss throughout the well. It is therefore necessary to derive a model that reflects the properties of the mud

as closely as possible. In such a model viscous properties, knows as rheology, and time-dependency, or thixotropy, are taken into account.

The gelling process of the mud has an important function in preventing the bit from becoming stuck. When the mud flow is shut down, all the cuttings will drop downwards due to gravity. Therefore, the use of gelled mud will lock the cuttings in the well, thereby reducing one of the risk factors that can cause a stuck bit.

The size of the cuttings will affect their removal process. Heavy (or large) particles will require increased transport velocities. Small particles, on the other hand, may modify the fluid viscosity, and facilitate the removal of the larger ones. These deposition phenomena were described by Newitt in 1955 in the model "Newitt's Classification of Slurry Pipeline Flow" (Figure 2.1), and his classification is still used (Bremer; 2008).

2.2.1   Rheology - The Bingham Plastic Model

The main functions of the mud are to transport cuttings up from the well without damaging the drilling device, as well as to act as a pressure control. As mentioned earlier, this fluid does not behave like a regular Newtonian fluid, but rather as a rigid body at low shear stress. However, as the stress increases, the material becomes more fluent. The Bingham Plastic Model is one of the rheological models for the drilling fluid and can be written as (Imsland; 2008)

$$\tau_w = \tau_0 + \mu_p \gamma \tag{2.1}$$

As can be seen from Eq. 2.1, there will be no fluid movement until a certain amount of stress is applied to the mud. This minimum amount of stress is referred to as τ_0 and is known as the yield point (see Fig. 2.2). If the value of the yield point (τ_0) is too low, cuttings will (due to gravity) increase the downhole pressure, which may cause damage to the drill bit. This value, along with the flow rate, should therefore be sufficiently high as to ensure that all the cuttings can be transported out of the well without causing damage to the
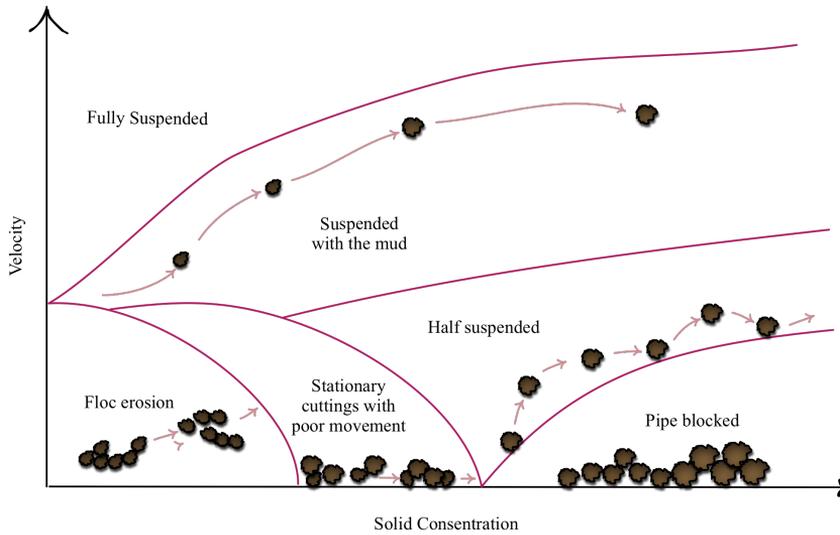
Figure 2.1: Newitt's Classification of Slurry Pipeline Flow (drawn with inspiration from (Bremer; 2008)). The illustration shows how the cuttings are removed with the mud. If the flow rate is too low, and the cuttings too big, the passage might get blocked.
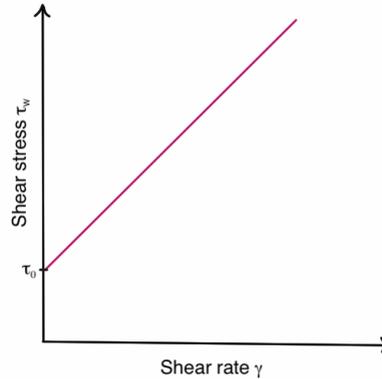
Figure 2.2: The theoretical reological behaviour of the Bingham plastic. The figure shows the yield stress τ_0.

drilling device. At the same time, the viscosity should be as low as possible, making a higher drill speed more attainable. In reality, the shear stress is not constant even though the shear rate is constant. If the pump is shut down, meaning there is no shear rate, the shear stress will continue to rise. When accounting for this, time-dependency has to be included in the model.

2.2.2 Thixotropy - Including build-up and break-down

As described in last years project (Swensen; 2013), the thixotrophy of a non-Newtonian fluid is a completely reversible process (Barnes; 1997), meaning that the fluid is able to go from one state to another - and back again.

When the fluid goes back and forth between high and low viscosity, two key mechanisms arise:

1. Build-up: caused by inflow collision.
   Brownian collisions [1] cause particles to fall into place (flocculation) and

---

[1] **Brownian motion**

Atoms move around randomly and collide with elements in the microstructure, which move

rebuild the structure. This process is referred to as gelling.

2. <u>Break-down:</u> caused by flow stress.
   When stress is applied to the structured mud, small flocs starts to secede, giving a shear thinning effect. This process is called floc erosion and is defined by "the particles of a dispertion form larger sized clusters." (UIPAC; 2011)

Equilibria

The thixotropic transformation can reach two equilibria as shown in Figure 2.3, one occurring when the fluid is as viscous [2] as possible (low viscosity) and one when the viscosity has reached the highest possible value (in the case of drilling mud, this state would be solid, locking the cuttings). Usually the build-up process takes far more time than the break-down (Barnes; 1997). In this project the build-up time is chosen to be approximately 70 times the break-down time.

Hysteresis

Because thixotrophy causes different build-up and break down times, the system can be in more than one internal state, depending on which states (solid or fluid) it comes from. This is referred to as *hysteresis* and can be defined as follows;

> "Hysteresis is the dependence of a system not only on its current environment but also on its past environment. This dependence arises because the system can be in more than one internal state"
> [Daniel A. Vallero (2013)]

As mentioned earlier, the gelling process is completely reversible, meaning that the drilling mud will not change properties after going back and forth between liquid and solid structures. The system may, however, have different

---

them to more favourable positions.(Hubbard; 2002)
  [2]**Viscosity**
High value: fluid more solid
Low value: thin fluid
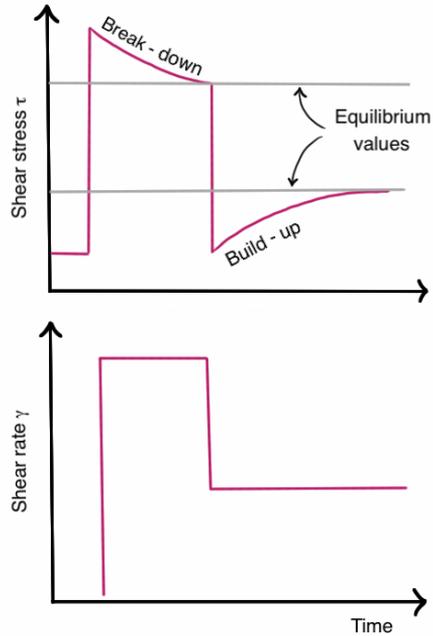
Figure 2.3: Figure drawn from (J. Sestak; 1982) to show the principles of the break-down and build-up for the fluid structure.

shear stresses for the same flow as shown in Figure 2.4, depending on the initial structure.

When the system initially starts from a solid structured state, it follows the purple line in Figure 2.4. When starting from a liquid state, on the other hand, decreasing the flow towards zero, it follows the green line. The values of shear stress for the green and the purple line are not identical for equal flow rates. This is called *rate-dependent* hysteresis and forms the loop illustrated in Figure 2.4. It is expected to see a tendency of hysteresis when simulating the system.

12
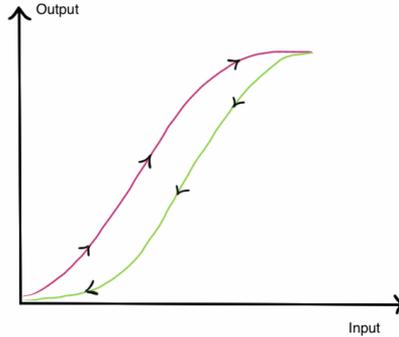
Figure 2.4: An illustration of the principles of hysteresis. The purple line shows a different output than that of the greenline, but they both start and end up in the same place.

Challenges

Mud at rest will, after some time, start the gelling process and rebuild its structure. When the system is to be set in motion again, a considerable amount of force is therefore needed in order to break the gel. However, a high degree of pressure from the pump may cause problems, such as bubbles (cavitations) that may erode the surface of the drillstring.

Another phenomenon that might cause trouble, or at least make the model less valid, is lubrication due to the non-linear break-down of the mud. During start-up of the rotation, shear stress from the wall will be the initial force acting on the mud. This will lead to lower viscosity close to the wall so that the mud will tend to function as a lubricant. The mud further from the wall will then be affected by less shear stress as the lubrication counteracts the break-down process. This dynamic is in the realm of advanced fluid mechanics and is not counted for in this project.

2.3 Pumps

This section presents the control of the two pumps in the system, the mud pump and the back pressure pump. Both of these are controlled in order to keep the downhole pressure constant. A P controller will be used as well as an approximation of the downhole pressure.

2.3.1 The Mud Pump

The mud pump provides drilling fluid to the drillstring. The deposition of the cuttings depends on the flow from the pump as well as the structural state of the mud.

When starting up after a shutdown, the mud will be more or less solid. If the pump provides a flow that is excessive, the pressure down hole will increase too fast causing large pressure peaks. These peaks might damage equipment as well as the environment.

The pump is principally controlled as follows:

> **Model 2.1:** Controlling the pumps (see Figure 2.5)
>
> 1. The control parameter is differentiated using a high pass filter.
> 2. A deadband distinguishes the largest peaks form the filtered signal.
> 3. The signal is compared to a desired rate of change, here zero.
> 4. The error is amplified by a P controller
> 5. If needed, the output is converted to $\frac{m^3}{s}$
> 6. The final signal is treated as disturbance to the reference flow q_p^{ref}

2.3.2 The Back Pressure Pump

The back pressure pump provides mud to the well when the main mud pump is shut down. This is to maintain the downhole pressure while a new drillstring
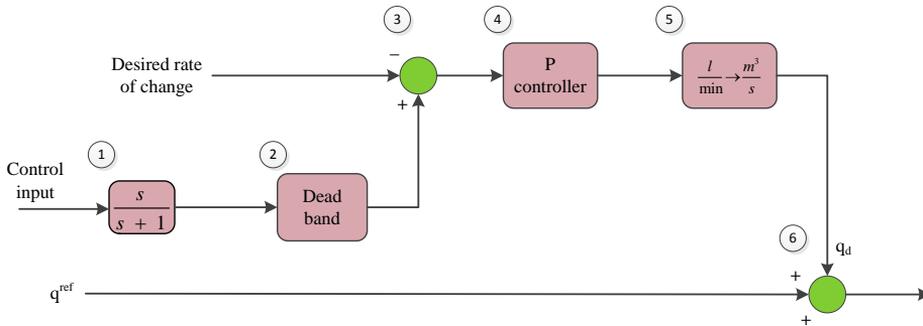
Figure 2.5: An illustration of the pump control according to Model 2.1

is being attached, or when there is some other reason for suspending drilling activity.

The mud provided by the pump is a constant flow treated as a disturbance to the choke flow. In this case, the pressure control is taken care of by the choke valve. When drilling, the back pressure pump is at rest.

Another option for increased pressure control would be to implement a P controller on the back pressure pump, making three control points.

2.4 Valves

2.4.1 Background

A drill rig usually consists of hundreds of valves. These are, for example, used for flow control, safety (blow out preventers), slower shut down or flow blocking. The most common valves used in drilling are check valves, control valves and gate valves (Valve; n.d.). A *gate valve* is usually formed like a disk and can cut through viscous liquids. These valves are only used to isolate sections of pipeline, not for adjusting the flow, meaning that they operate in a fully open or fully closed position (tyco Water; n.d.). A *check valve*, which will be described

in more detail in Section 2.4.3, is a one-way valve used to prevent flow from going backwards. Therefore, the valve usually used to <u>control</u> the mud flow, is a *control valve*. These valves are often known by different names, depending on how much detail needs to be conveyed. Some examples of control valves used in drilling are globe valves, choke valve or flanged angle-style control valves (Management; 2005).

Today's technology allows for control valves to be equipped with several measurement tools, such as position indicator, a digital pump rate meter, or a timer (MiSwaco; 2013). Thus the valves might, for example, have the ability to control the mud pump startup and shutdown, the making and breaking of drillpipe connections, as well as automatically adjusting the orifice size.

2.4.2 How the choke valve works

Basics

The basic principle of a choke valve is that it has a moveable disk type element (the sliding shuttle shown in Fig. 2.6) that can be put in specific positions in order to obtain desirable flow. The valve consists of an actuator [3], a positioner [4] and a body. Choke valves are constructed such that cuttings and other obstacles can pass through without becoming stuck.

When calculating the flow through the choke valve, the Bernoulli equation (White; 2008) is used

$$p_1 + \frac{1}{2}\rho v_1^2 + \rho g h_1 = p_2 + \frac{1}{2}\rho v_2^2 + \rho g h_2 \tag{2.2}$$

The schematic in Figure 2.6 shows a hypothetical choke valve used to choke the mud flow. Using the figure, along with Eq. 2.2, and assuming that $h_1 = h_2$ and

---

[3]**Actuator**: A pneumatic, hydraulic, or electrically powered device that applies force and motion to open or close a valve.(Management; 2005)

[4]**Positioner**: Automatically adjust the output of the actuator to maintain a desired position according to the input signal.(Management; 2005)
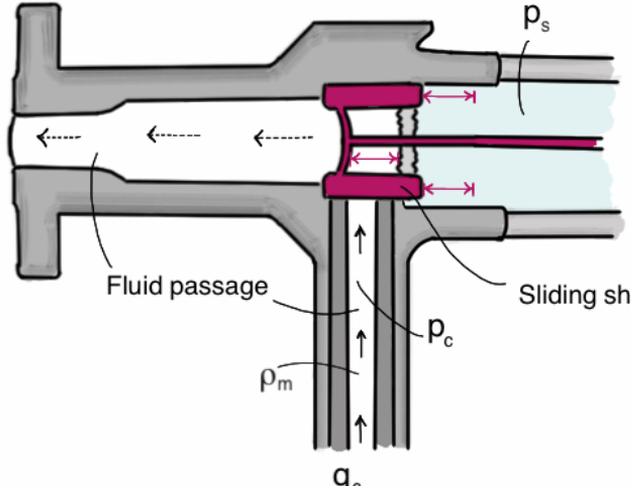
Figure 2.6: Illustration of a choke valve. Used to describe the principles behind the choke flow model. Figure is drawn following (MiSwaco; 2013)

$v_2 = q_s = 0$, one obtain

$$p_c + \frac{1}{2}\rho_m q_c^2 + \overbrace{\rho_m g h_1}^{} = p_s + \overbrace{\frac{1}{2}\rho q_s^2}^{=0} + \overbrace{\rho g h_2}^{} \tag{2.3}$$

$$p_c + \frac{1}{2}\rho_m q_c^2 = p_s \tag{2.4}$$

Solving for q_c

$$\frac{1}{2}\rho_m q_c^2 = p_c - p_s \tag{2.5}$$

$$q_c^2 = \frac{2}{\rho_m}(p_c - p_s) \tag{2.6}$$

$$q_c = \sqrt{\frac{2}{\rho_m}(p_c - p_s)} \tag{2.7}$$

17

2.4.3 The check valve

Several types of check valves are used in pipes. The ball valve seems to be the most convenient valve to use in a drillbit and is therefore chosen to be further described in this project.

When modelling, an extra condition ($max[0, \cdot]$ for $q_b = 0$) in Eq. (3.3) will be added. This is because it is assumed that there is a check valve in the drill bit (see Figure 2.7). A ball in the fluid passage can freely be moved by the mud between the front and the rear seat. When drilling, the mud flows downwards from the mud pump and through the bit. The ball will then be situated at the front seat. As long as the length of B is larger than the diameter of the ball, the fluid will run without being affected. When the drilling stops, the mud pump is turned off. If the downhole pressure is larger than the pressure in the fluid passage in the drill bit, there will be a backflow. This backflow will push the ball to the rear seat, sealing the pipe.

The ball will move back and forth between the surfaces frequently and can cause heavy wear and tear. For this reason it is usually made out of soft/elastic materials (Bengt Aberg; 1997).
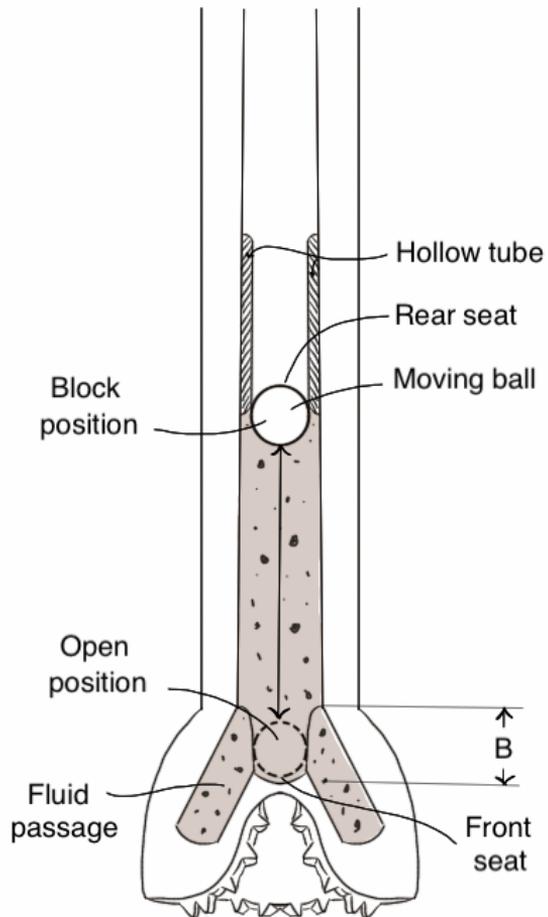
Figure 2.7: Illustration of a check valve in the drill bit (drawn from (Bengt Aberg; 1997)).

2.5 Pressure Control Using P and PI controllers

In this project P controllers are used for pump flow control and PI controllers for valve control. A derivative action does not appear to provide any further improvement of the system.

2.5.1 Why not a PID controller?

In this project a PI-controller is used. It contains two terms, the proportional term and the integral term. It is usually expected that a PID controller would be used, but for this project, it is not considered suitable. The main reason is simply that there is no need for it and, another is that it would probably harm the system and cause damage to the valve. The controller works as follows.

The illustration in Figure 2.8 shows a variable signal along with a reference line. The proportional gain delineates to how far from the gain the signal is. As the signal moves further away from the reference line, the proportional term will increase, which can be seen from Eq. (2.8) . When the signal approaches the setpoint value, the proportional term will be very small, but never reach zero.

$$P_{PI} = K_p(y^{ref} - y) \qquad (2.8)$$

The integral action, I_{PI}, ensures that the signal spends the same amount of time on each side of the set point (Welander; 2010), or more precisely, it keeps track of the total area on each side of R_{PI} (Eq. 2.9). For every moment the signal is at one side of the set point, I_{PI} increases. In order for I_{PI} to decrease, the signal has to pass the set point and stay there for the same amount of time.

$$I_{PI} = K_i \int_0^t (y^{ref}(\tau) - y(\tau))d\tau \qquad (2.9)$$

The derivative action, D_{PI}, is described as in Eq. 2.10 and has no direct impact on the signal. The only action D_{PI} has is to counteract the other control signals; the more the control signal changes, the more effort D_{PI} will put in to
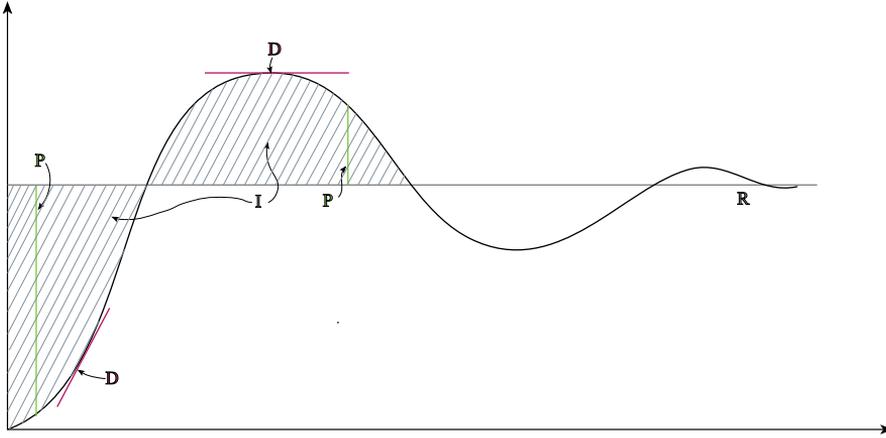
Figure 2.8: Illustration of the terms of a PID controller. The proportional term are marked as green lines, showing the distance from the reference. The blue shading are the area added up by the integral term. The derivative term are marked as purple tangents to the curve, where the slope are the derivative value.

slowing down. This is an advantage if overshoots are crucial. If I_{PI} becomes too eager to get the signal on the other side of R_{PI}, D_{PI} will act as a damper such that it more slowly reaches the R_{PI}.

$$D_{PI} = K_d \frac{d}{dt}(y^{ref}(t) - y(t)) \tag{2.10}$$

Every time the signal has been too long on one side of R_{PI} or too far from R_{PI}, I_{PI} and P_{PI}, respectively, increases. Whenever this happens fast enough, D_{PI} will try to damp the control effect. This is somewhat similar to driving a car with one foot on the accelerator and one foot on the brake at the same time.

’A well-tuned PI controller is going to beat a moderately tuned PID controller every time. Adding the extra tuning parameter adds com-

plexity, which can confuse a lot of people. It's only in those remain-
ing percentage points where you've got a really slow loop but you
can't afford MPC.'

Bob Rice, Ph.D., director of solutions engineering for Control Sta-
tion

Windup

In reality there will be constraints (max opening, max speed etc.)on the control
signal (Eq. 3.3), meaning that it saturates before it reaches R_{PI}. This makes
I_{PI} run wild because of the time spent below R_{PI}. I_{PI} will not decrease again
before the same amount of time is spent above R_{PI}, which might never happen.
This windup makes the whole system uncontrollable. Because I_{PI} increases
for every moment below the line, it has to be reset from time to time, such
that it does not grow beyond boundaries. This reset procedure is known as
'anti-windup'.

There are several anti-windup methods, which are incremental, conditional
integration, observer appoach and back-calculation (Bemporad; 2010). How-
ever, only back-calculation will be considered in this project. The back-calculation
subtracts the signal before saturation from the signal after saturation (see Fig.
2.8). When the signal does not saturate, this difference will be zero. When in
saturation the difference will be amplified and added to the error fed into the
integrator.
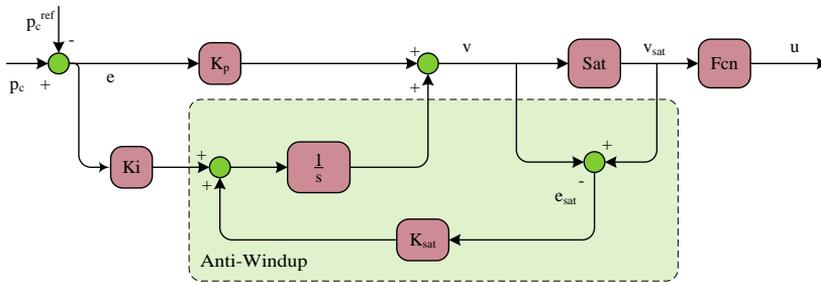
Figure 2.9: Block diagram showing the principle of *anti-windup*. The signal before and after saturation is subtracted, amplified and added to the integral gain.

3 | Modelling

3.1 A standard MPD system

Standard MPD systems nowadays contains a choke valve as well as a back pressure pump to control the bottomhole pressure. This section will therefor present an MPD system with a constant input flow, a choke valve with a controller, and a back pressure pump, as well as a realistic model of the drilling fluid.

Below is an overview of the model derived in this section. An overview of the total system can be seen in Table 3.1 on page 39.

Model 3.1: The Standard MPD Model

$$\frac{V_d}{\beta_d} \dot{p}_p = q_p - q_b \tag{3.1}$$

$$\frac{V_a}{\beta_a} \dot{p}_c = q_b - q_c + q_{bpp} \tag{3.2}$$

$$[M_d + M_a]\dot{q}_b = \begin{cases} p_p - p_c - \Delta p_f - \Delta p_{other} & q_b > 0 \\ max[0, p_p - p_c - \Delta p_f - \Delta p_{other}] & q_b = 0 \end{cases} \tag{3.3}$$

$$p_{dh} = p_c + \Delta p_{f,a}(q_b, L_a) + \rho_m g h_a \tag{3.4}$$
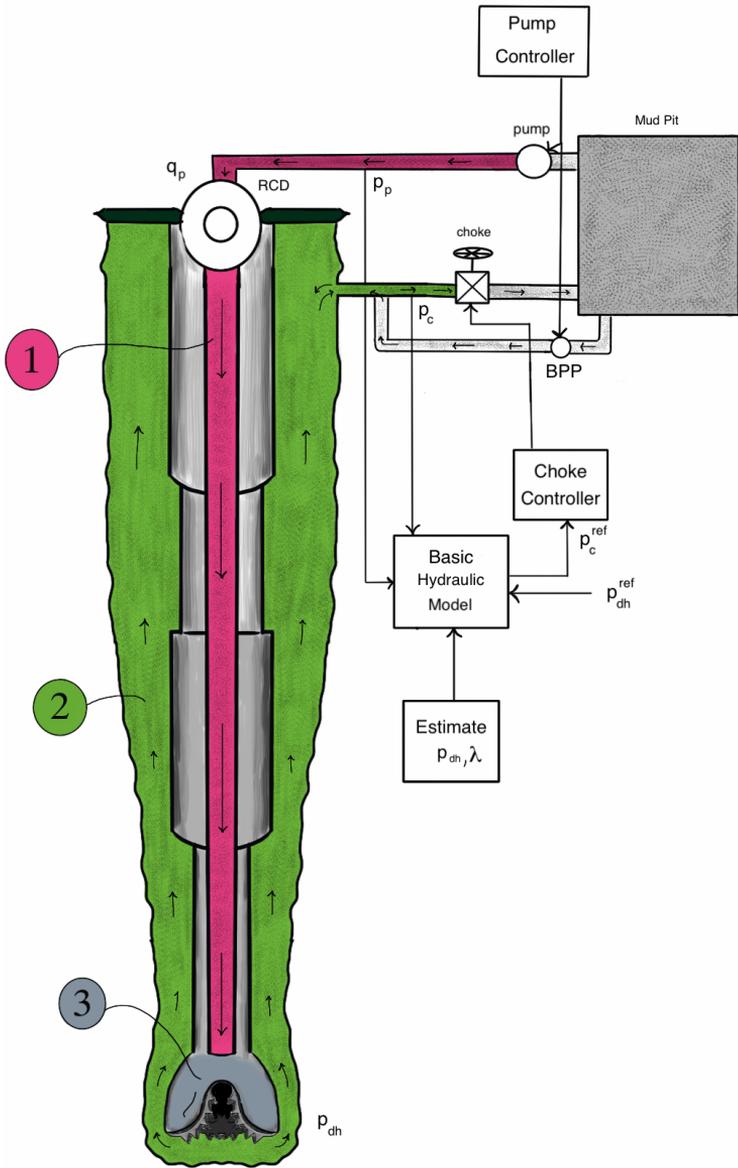

Figure 3.1: Control volumes

3.1.1 The Base: A Hydraulic Model

The whole system used in this project is based on a hydraulic model defined by (Kaasa 2012). The model describes the flow dynamics through the system and consists of three state equations, each representing one control volume. An overview of the equations is found in Table 3.1 on page 39.

Overview

When modelling the mud flow through the drilling device, three control volumes according to Figure 3.1 are selected:

1 The pipe, described by the flow difference between the mud pump and the drill bit.
2 The annulus, described by the flow difference between the drill bit and the choke valve.
3 The bit, described by the pressure difference between the mud pump and the choke valve including friction loss.

In order to obtain as simple a model as possible several dynamics are excluded

- Rotation of drillstring
- Rotation of the drilling bit
- Temperature
- Size of cuttings
- Volume changes (lack of mud, heave motions)
- Turbulent flow
- Wear and tear of equipment
- Roughness of surface

From last year's project (Swensen; 2013) the three control volumes were used to implement a simplified hydraulic model. The model is a third order system which describes the rate of change in the pump pressure ($\dot{p}_p$), the choke pressure ($\dot{p}_c$) and the bit flow ($\dot{q}_b$).

Deriving the model

Control volume 1

From (Kaasa 2012) the conservation of mass, along with the conservation of momentum, was used to put up the pressure behavior

$$\frac{d}{dt}(\rho V) = w_{in} - w_{out} \tag{3.5}$$

$$= \rho_{in} q_{in} - \rho_{out} q_{out} \tag{3.6}$$

$$V\dot{\rho} + \overbrace{\rho \dot{V}}^{=0} = \rho_{in} q_{in} - \rho_{out} q_{out} \tag{3.7}$$

where $d\rho = \frac{\rho_0}{\beta} dp$ (Kaasa 2012) and assuming constant control volume, $\frac{dV}{dt} = 0$.

$$V\frac{\rho_0}{\beta}\dot{p} = \rho_{in} q_{in} - \rho_{out} q_{out} \tag{3.8}$$

When assuming equal mud densities ($\rho_0 = \rho_{in} = \rho_{out}$), they will cancel out. The pressure model will then be

$$\frac{V_{CV}}{\beta_{CV}}\dot{p} = q_{in} - q_{out} \tag{3.9}$$

Applying this to the first control volume, the drillstring, using the pump flow as input and the bit flow as output

Pump Pressure Equation

$$\frac{\mathbf{V_d}}{\beta_\mathbf{d}}\dot{\mathbf{p}}_\mathbf{p} = \mathbf{q_p} - \mathbf{q_b} \tag{3.10}$$

where V_d (calculated in Table A) is the volume of the drillstring and β_d is the bulk modulus for the fluid in the drillsting.

28

Control volume 2

The derivation of the equation for the choke pressure is the same as for the pump pressure in the previous section. The bit flow, as well as the flow from the back pressure pump, is used as an input flow. The output will be the choke flow. Also, the volume and the bulk modulus have to be for the annulus rather than for the drillstring. Using Eq (3.7) for the second control volume

$$V_a\dot{\rho} + \overbrace{\rho\dot{V_a}}^{=0} = \rho_{in}q_a - \rho_{out}q_a \tag{3.11}$$

$$V_a\frac{\rho_0}{\beta}\dot{p}_c = \rho_{in}q_b - \rho_{out}q_c \tag{3.12}$$

where, in this project, the annulus volume is kept constant. Dynamics that might change the annulus volume are heave motion (when drilling in water), borehole washout or pack-off (Rasmus; 2013). The resulting model for the choke pressure is then

---

Choke Pressure Equation

$$\frac{\mathbf{V_a}}{\beta_\mathbf{a}}\dot{\mathbf{p}}_\mathbf{c} = \mathbf{q_b} + \mathbf{q_{bpp}} - \mathbf{q_c} \tag{3.13}$$

where V_a and β_a are the volume and the bulk modulus for the fluid in the annulus, respectively (Table A). q_c is controlled by a choke valve (Section 2.4.2). q_{bpp} is further described in Section 3.1.2.

Control volume 3

The equation for an average flow rate is described by Eq. (18) in (Kaasa 2012)

$$M(l_1, l_2)\frac{dq}{dt} = p_1 - p_2 - F(l_1, l_2, q, \mu) + G(l_1, l_2, \rho) \tag{3.14}$$

The bit flow is assumed to be the average flow between the mud pump and the choke valve, including friction loss. The model will then be

$$M(l_{pump}, l_{choke})\dot{q}_b = p_p - p_c - F(l_{pump}, l_{choke}, q_b, \mu_p) + G(l_1, l_2, \rho_m) \tag{3.15}$$

where M is the integrated density per cross-section over the flow path. The values are taken from Imsland (2008) such that $M(pump, choke) = M_d + M_a$. $F(\cdot)$ is the pressure loss due to friction and is divided into two parts, one for the drillstring ($\Delta p_{f,d}(q_b, L_d)$) and one for the annulus ($\Delta p_{f,a}(q_b, L_a)$). These can be summed up as Δp_f and will be described in greater details in Section 3.1.2. $G(\cdot)$ is the total gravity affecting the fluid. Assuming that the mud pump and the choke valve are situated at the same level (see Figure 3.1), or close enough as not to have any significant effect, the total gravity affecting the fluid will be zero. Hydrostatic pressure loss is also ignored because it will have only a minor effect compared to the friction loss (Imsland; n.d.).

Other pressure losses will occur, such as pressure loss in the surface connections (Δp_{sc}), drill bit (Δp_b) and downhole tools (Δp_{dt}). These losses are summed up as Δp_{other}.

Using the above assumptions to rewrite Eq. (3.15)

$$(M_d + M_a)\dot{q}_b = p_p - p_c - \Delta p_f - \Delta p_{other} \tag{3.16}$$

When the mud pump is shut down, eg. due to drillstring extension, a check valve (as described in Section 2.4.3) ensures that no fluid returns to the drillstring. Therefore one more condition (when $q_b = 0$) needs to be added to Eq. 3.16

Bit Flow Equation

$$(\mathbf{M_d} + \mathbf{M_a})\dot{\mathbf{q}_b} = \begin{cases} \mathbf{p_p} - \mathbf{p_c} - \mathbf{\Delta p_f} - \mathbf{\Delta p_{other}} & q_b > 0 \\ \mathbf{max}[\mathbf{0}, \mathbf{p_p} - \mathbf{p_c} - \mathbf{\Delta p_f} - \mathbf{\Delta p_{other}} & q_b = 0 \end{cases} \tag{3.17}$$

where p_p and p_c are the pump and choke pressure, respectively, derived above. Δp_f is the pressure loss due to friction, derived in Section 3.1.2 and Δp_{other} is the pressure drop due to other dynamics. These can also be found in Section 3.1.2.

3.1.2 Extending the Model

Pressure Losses

When the mud flows through the system, several pressure losses affect the down-hole pressure. In this section the friction models will be presented as well as other pressure losses.

The pressure loss due to friction is modelled as

$$\Delta p_f = \overbrace{\Delta p_{f,d}(q_b, L_d)}^{\text{drillstring}} + \overbrace{\Delta p_{f,a}(q_b, L_a)}^{\text{annulus}} \tag{3.18}$$

while the pressure loss due to other dynamics are

$$\Delta p_{other} = \overbrace{\Delta p_{sc}}^{\text{surface connections}} + \overbrace{\Delta p_b}^{\text{bit}} \tag{3.19}$$

Pressure loss due to friction

The friction terms $\Delta p_{f,d}(q_b, L_d)$ and $\Delta p_{f,a}(q_b, L_a)$ may be modelled in several ways, as shown in Figure 3.2, depending on the properties of the mud. The simplest way, in order to obtain an overview of the system, will be to just add a quadratic friction term

$$\Delta p_f = f q_b^2 \tag{3.20}$$

where f is a constant found by

$$f = \frac{p_{p,ss}}{q_{b,ss}^2} \overbrace{\cdot 1000 \cdot 60}^{lpm \rightarrow \frac{m^3}{s}} \tag{3.21}$$

Here $p_{p,ss} = 188.1$ bar and $q_{b,ss} = 2000$ lpm. A multiplication by $1000 \cdot 60$ is done in order to convert from lpm to $\frac{m^3}{s}$.

Using this simple form might be an effective way to test the dynamics of the system before adding more complex friction models. Furthermore, unknown friction can be modelled using a quadratic term, but it should be noted that
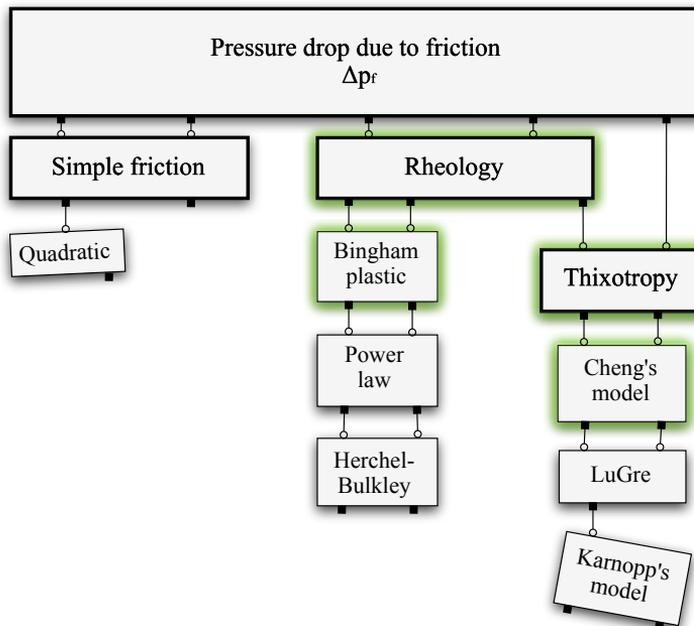
Figure 3.2: Diagram showing the levels of friction. The models used in this project are shown in green.

this might cause trouble for low flow rates ($q_b \simeq 0$).

The mud used in drilling is viscous, therefore a better approach would be to add a rheological friction model, e.g. the Bingham plastic model. When taking the muds ability of gelling, adding time-dependency to the model will enhance its realism. Friction models, including time-dependency would be the LuGre model (Imsland; 2008), Karnopp's model (Olav Egeland; 2002) or the Cheng model (J. Sestak; 1982). In this project the Cheng model is used and is described in further details in Section 3.1.2 on page 34.

When adding the properties for the viscous mud, the pressure drop due to friction can be defined as (Imsland; 2008)

> **Model 3.2:** Frictional pressure loss for a time dependent Bingham plastic
>
> $$\Delta p_f = \frac{4}{\pi}\tau_w \qquad (3.22)$$
>
> where τ_w is from the Cheng model (Eq. 3.30).

Other Pressure Losses

The mud passes several obstacles on its way through the system. The most important pressure losses to be included are (Imsland; 2008):

- Pressure loss due to surface connections

$$\Delta P_{sc} = C_{sc}\rho_m \frac{q_b}{100}^{1.86} \qquad (3.23)$$

- Pressure loss in drill bit

$$\Delta p_b = \frac{\rho_m}{2C_d^2 A^2}q_b^2 \qquad (3.24)$$

where C_{sc}, C_d are constants in Table A.1. The density is found by

$$\rho_m = g_s \rho_{H_2O} \qquad (3.25)$$

Modelling Thixotropy

The working parameter $\frac{d\lambda}{dt}$

The thixotropic model includes time-dependency as well as a description of the state of the microstructure (viscosity). The viscosity of the mud is described by a factor λ, which is a number between 0 and 1. A value close to 0 represent low viscosity and vice versa. Time-dependency is introduced in the working parameter $\frac{d\lambda}{dt}$. Negative values signify that the structure is breaking down, while high values represent the build-up phase, gelling. The working parameter is expressed as follows:

$$\frac{d\lambda}{dt} = g(\gamma, \lambda) \qquad (3.26)$$

where (Imsland; 2008)

$$\gamma = \frac{8}{d}v, \quad \text{and} \quad v_p = \frac{4}{\pi}\frac{1}{d_i^2}q_b, \quad v_a = \frac{4}{\pi}\frac{1}{(d_h - d_o)}q_b \qquad (3.27)$$

Time Dependent Yield Stress

The simplest model used when introducing time dependency into the rheological model is Tiu-Boger J. Sestak (1982)

$$\tau = \lambda(\tau_0 + \mu_p\gamma) \qquad (3.28)$$

This model has shown itself to be too simple because of the lack of sufficient accuracy when it comes to the break-down/build-up phase and anomalous behavior. Therefore, Cheng's model for thixotrophy on the next page is used.

The shear stress can also be written

$$\tau_q = \tau_0 + \tau_1\left(\lambda - \frac{a}{a + b\gamma}\right)e^{-(a+b\gamma)t} + \mu_p\gamma \qquad (3.29)$$

It can be seen that when $t \to \infty$, the model for a Bingham plastic in Eq. 2.1 is achieved.

For the sake of simplicity the model in the form of Eq. 3.30 will be used in

simulations. Otherwise, t would have to be reset every time the gelling process changes (because of the term $e^{-(a+b\gamma)t}$), which may be somewhat inconvenient.

The Cheng model for thixotropic behavour

$$\tau_w = \tau_0 + \tau_1\lambda + \mu_p\gamma \tag{3.30}$$

$$\frac{d\lambda}{dt} = a(1-\lambda) - b\gamma\lambda \tag{3.31}$$

where γ is as in Eq. and J. Sestak (1982)

$$\tau_0 = 0 \text{ Pa}, \quad \tau_1 = 21.5 \text{ Pa}, \quad a = 1 \cdot 10^{-3}\frac{1}{s}, \quad b = 1.44 \cdot 10^{-5}$$

The Choke Flow, q_c

A standard equation for the choke (Eq. 2.7) was derived in the theory section:

$$q_c = \sqrt{\frac{2}{\rho_m}(p_c - p_s)} \tag{3.32}$$

In order to obtain a valve size used in current drilling rigs, some further parameters are added.

Fitting the choke valve to realistic dimensions

A valve model was provided from Statoil (Kittelsen)

$$q_c = kC_v\sqrt{\frac{\Delta p}{\rho}} \tag{3.33}$$

where C_v is a *flow coefficient* and k[1] is a numerical constant used for valve fitting. C_v is related to the geometry of the choke valve. It is used to determine the characteristics of the flow as a function of the percentage of valve travel

---

[1]When modelling, different units might appear within the equations. Therefore, when the flow is given in $\frac{m^3}{min}$ and the pressure is given in Pa, the spesific constant $N_1 = 0.0865 = k$ from the table at p. 113 in Management (2005) is used.
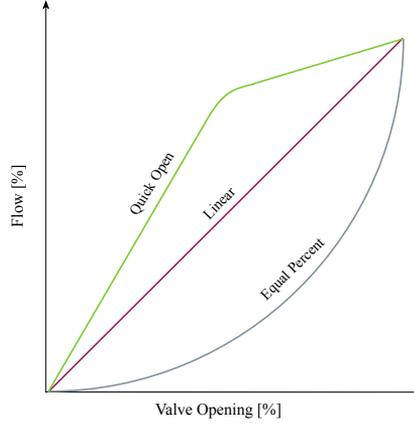
Figure 3.3: Figure showing the choke characteristics from (Management; 2005).

versus percentage of flow. In Figure 3.3 three different valve charateristics are demonstrated (Management; 2005), where the linear valve characteristics are to be implemented.

The resulting model, using Eq. 3.32 and 3.33, for the choke valve, with a controller g(u), is then

Choke Valve Equation

$$q_c = kC_v\sqrt{\frac{p_c - p_s}{\rho_m}}g(u) \tag{3.34}$$

where the controller g(u) will be described below.

The PI Controller

The PI controller used for the choke is implemented as follows:

$$u(t) = K_p e(t) + K_i e(t)\frac{1}{s} \tag{3.35}$$

where $K_p = 0.05$, $K_i = 0.003$ (Landet; 2010) and $e(t) = p_{dh}^{ref} - p_{dh}$.

Approximation towards reality

In this project, the choke which is to be controlled, has limitations. It cannot be less than closed and it can not be more than open, ie $0 < u < 1$. In (Swensen; 2013), the choke opening was modelled with unlimited opening capacity, whereas in reality, this is not the case. Therefore, a saturation block is added constraining the output such that $0 < u < 1$. Additionally, the choke can not go instantaneously from closed to fully open as it takes approximately 30 second for it to open (Imsland; n.d.). In order to limit the rate of change a low-pass filter with a time constant T_c is implemented as follows

$$t = T_c \frac{du}{dt} + u$$
$$= T_c s u + u$$
$$= u(T_c s + 1)$$
$$y = u$$

then

$$H(s) = \frac{y}{u} = \frac{u}{u(T_c s + 1)} = \frac{1}{T_c s + 1} \tag{3.36}$$

T_c is found by taking the time u needs to reach 63% of the desired value over a time period of 30 seconds.

$$T_c = \frac{30sec \cdot 63\%}{100\%} = 18.9sec \tag{3.37}$$

The low-pass filter, acting as a rate limiter, is multiplied by the signal from the saturation block (Figure 3.4).

Anti-windup

A saturation in combination with a constraint on the choke opening ($0 \leq u \leq 1$) will cause heavy windup every time the contoller are unable to reach the reference (saturation) in a sufficiently short time. The integrator starts to wind up for every instant that the saturation is in progress. Therefore, an anti-windup back-calculation loop is created (lower part of Figure 3.4). The anti-windup loop resets the integrator, making the integral term "forget" for how long the error has been positive.
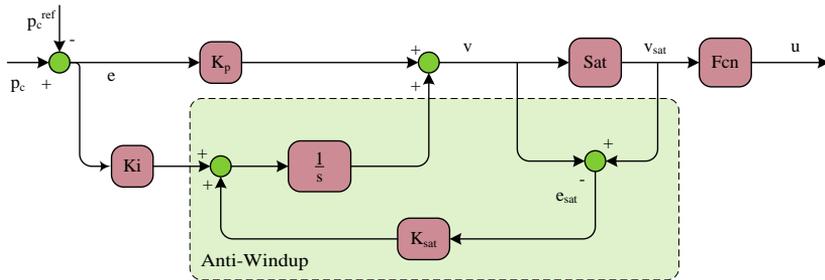

Figure 3.4: The PI controller with anti-windup. The output of the controller is first saturated (limiting choke opening) and then low pass filtered (limiting rate of change for the choke).

The Back Pressure Pump

The back pressure pump is modelled as a constant flow, which is turned on when the mud pump is shut down.

$$q_{d,BPP} = b(q_p^{ref})K_{BPP} \qquad (3.38)$$

where

$$b(q_p^{ref}) = \begin{cases} 0 & , & q_p^{ref} \neq 0 \\ 1 & , & q_p^{ref} = 0 \end{cases} \qquad (3.39)$$

Standard MPD System Overview	
State equations	$\frac{V_d}{\beta_d}\dot{\mathbf{p}}_{\mathbf{p}} = q_p - q_b$ $\frac{V_a}{\beta_a}\dot{\mathbf{p}}_{\mathbf{c}} = q_b - q_c + q_{bpp}$, where q_c is the controller $[M_d + M_a]\dot{\mathbf{q}}_{\mathbf{b}} = \begin{cases} p_p - p_c - \Delta p_f - \Delta p_{other} & q_b > 0 \\ max[0, p_p - p_c - \Delta p_f - \Delta p_{other}] & q_b = 0 \end{cases}$ $q_c = kC_v\sqrt{\frac{p_c - p_s}{\rho_m}}g(u)$
Pressure losses	$\Delta p_f = \Delta p_{f,d} + \Delta p_{f,a}$ $\Delta p_{f,d} = \frac{4}{d_i}\tau_w$ $\Delta p_{f,a} = \frac{4}{d_h - d_o}\tau_w$ $\Delta p_{other} = \Delta p_{sc} + \Delta p_b$ $\Delta p_{sc} = C_{sc}\rho_m \frac{Q}{100}^{1.86}$ $\Delta p_b = \frac{\rho_m}{2C_d^2 A^2}q_b^2$
Cheng's Model	$\tau_w = \tau_0 + \tau_1\lambda + \mu_p\gamma$ $\frac{d\lambda}{dt} = a(1 - \lambda) - b\gamma\lambda$
Controller	$$g(u) = \overbrace{(K_p + K_i\frac{1}{s})(p_c - p_c^{ref})}^{PI} \cdot \overbrace{sat(0,1) \cdot \frac{1}{T_c s + 1}}^{\text{Opening and rate limit}} \cdot(\text{anti-windup})$$
Downhole Pressure	$p_{dh} = p_c + \Delta p_{f,a}(q_b, L_a) + \rho_m g h_a$

Table 3.1: Overview of the standard MPD system. Constants can be found in App. A

3.2   An Extended MPD System

This section presents an MPD system with two control devices, the choke valve and the mud pump. The mud pump controller will be presented, as well as a suggestion for a controller for the back pressure pump.

The MPD system in Section 3.1 contained one automated device, the choke valve. In order to obtain even more control when starting up after a shutdown, it might be convenient to incorporate an automated mud pump.

3.2.1   Controlling the Mud Pump

Two P controllers are used to control the flow from the mud pump, one monitoring the downhole pressure, the other useing an estimate of the structural state of the mud. The inputs of each of these controllers are therefore

1. the rate of change of p_{dh}

2. the rate of change of the working parameter $\frac{d\lambda}{dt}$

The output from the controllers are added and used as a disturbance on the reference pump flow:

Mud Pump Flow
$$q_p = q_p^{ref} - q_{d,p_{dh}} - q_{d,\lambda} \qquad (3.40)$$

where $q_{d,p_{dh}}$ is described by Eq. 3.41 and $q_{d,\lambda}$ by Eq. 3.42

The control structure was presented in the theory section and is shown again in Model 3.3. Below is a more detailed description of how the controllers work.

Controller 1 – Downhole Pressure

Control input:	p_{dh}
Desired rate of change:	0
Added to:	q_b^{ref}

Model 3.3: Mud Pump Controller

1. The control parameter is differentiated using a high pass filter.
2. A deadband distinguishes the largest peaks form the filtered signal.
3. The signal is compared to a desired rate of change, here zero.
4. The error is amplified by a P controller
5. If needed, the output is converted to $\frac{m^3}{s}$
6. The final signal is treated as disturbance to the reference flow q_p^{ref}
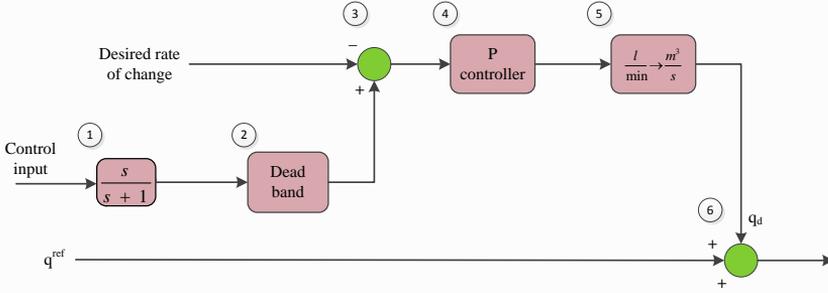
The first controller monitors the rate of change in the downhole pressure, and use the signal as a control parameter. By adding a high pass filter as a differentiator, it is possible to distinguish periods during which the pressure increases too fast.

When the high pass filter is functions as a differentiator, only inputs with a rate of change larger than $\frac{1}{\tau}$ will pass without changes. Signals containing smaller changes will be suppressed and are not visible on the output. This approach to selecting parts of the signal, makes it possible to adjust the pump flow only when needed.

The pump is modelled according to Model 3.3. For convenience, the s-domain is used:

$$q_{d,p_{dh}} = \left(\frac{s}{s+1} p_{dh} \overbrace{f_{d,p_{dh}}(u)}^{deadband} - (sp_{dh})^{ref} \right) K_{p,p_{dh}} \qquad (3.41)$$

where

$$f_{d,p_{dh}}(u) = \begin{cases} 0 & , & -\infty < u < 0.05 \\ 1 & , & \text{otherwise} \end{cases} \quad , \quad \dot{p}_{dh}^{ref} = 0 \quad \text{and} \quad K_{p,p_{dh}} = 500$$

The pump model in the time domain is somewhat more complicated and less intuitive, and is therefore omitted. If wanted, the moden in time domain is found by applying a Laplace transform to the above model.

Controller 2 – Mud Structure

Control input:	$\frac{d\lambda}{dt}$
Desired rate of change:	0
Added to:	q_b^{ref}

In order to suppress the downhole pressure peaks even more, it might be worthwhile to look at the mud structure in addition to the downhole pressure. Modeover, it is assumed that the structure of the mud is possible to predict using a mathematical model.

The controller takes the working parameter, $\frac{d\lambda}{dt}$, as an input. Even though the point is to obtain a viscous mud as fast as possible, the desired effect is to ease down the flow rate whenever the process of break-down develops too fast. This is because a fast break-down inticates an excessively increasing rate of the pressure down hole.

As for the previous controller, the input signal is differentiated using a high pass filter. The highest peaks are then amplified by a P controller as shown in Model 3.3, which are used as a disturbance to the mud pump flow. The model can be written in the s-domain as follows:

$$q_{d,\lambda} = \left(\frac{s}{s+1} s\lambda f_{d,\lambda}(u) - (s^2\lambda)^{ref} \right) K_{p,\lambda} \tag{3.42}$$

where

$$f_{d,\lambda}(u) = \begin{cases} 0 & , \quad -3 \cdot 10^{-5} < u < \infty \\ 1 & , \quad \text{otherwise} \end{cases} \quad , \quad (s^2\lambda)^{ref} = 0 \quad \text{and} \quad K_{p,\lambda} = 25 \cdot 10^6$$

3.2.2 Controlling the Back Pressure Pump

For the standard MPD system in Section 3.1 the back pressure pump provided a constant flow rate, starting simultaneously as the mud pump shutdown. Another approach for improved pressure control might be to apply automatic control to the pump, with the downhole pressure as a control parameter.

The Controller

Control input:	p_{dh}
Desired rate of change:	0
Added to:	q_c

When controlling the back pressure pump, a regular P controller is used:

$$q_{d,bpp} = (p_{dh}^{ref} - p_{dh})K_{p,bpp} \overbrace{sat(q_{bpp_{low}}, q_{bpp_{high}})}^{\text{flow limitation}} \tag{3.43}$$

where

$$p_{dh}^{ref} = p_c^{ref} + \rho_m g L_a * G_{BPP}(q_p^{ref})g_{BPP} \tag{3.44}$$

and

$$g_{BPP} = 25 \quad , \quad G_{BPP}(q_p^{ref}) = \begin{cases} 1 & , \quad \text{for } q_p^{ref} = 0 \\ 0 & , \quad \text{else} \end{cases} \tag{3.45}$$

As can be seen from Eq. (3.44), the reference pressure will depend on the well depth. The function $G_{bpp}(q_p^{ref})$ works as a switch; when the mud pump is shut down, the back pressure pump starts up.

	Advanced MPD System Overview
State equations	$\frac{V_d}{\beta_d}\dot{\mathbf{p}}_{\mathbf{p}} = q_p(p_{dh,\lambda}) - q_b$ $\frac{V_a}{\beta_a}\dot{\mathbf{p}}_{\mathbf{c}} = q_b - q_c$, where q_c is the controller $[M_d + M_a]\dot{\mathbf{q}}_{\mathbf{b}} = \begin{cases} p_p - p_c - \Delta p_f - \Delta p_{other} & q_b > 0 \\ max[0, p_p - p_c - \Delta p_f - \Delta p_{other}] & q_b = 0 \end{cases}$ $q_c = kC_v\sqrt{\frac{p_c - p_s}{\rho_m}}g(u)$
Pressure losses	$\Delta p_f = \Delta p_{f,d} + \Delta p_{f,a}$ $\Delta p_{f,d} = \frac{4}{d_i}\tau_w$ $\Delta p_{f,a} = \frac{4}{d_h - d_o}\tau_w$ $\Delta p_{other} = \Delta p_{sc} + \Delta p_b$ $\Delta p_{sc} = C_{sc}\rho_m\frac{Q}{100}^{1.86}$ $\Delta p_b = \frac{\rho_m}{2C_d^2 A^2}q^2$
Cheng's Model	$\tau_w = \tau_0 + \tau_1\lambda + \mu_p\gamma$ $\frac{d\lambda}{dt} = a(1-\lambda) - b\gamma\lambda$
Choke Valve Controller	$g(u) = \overbrace{(K_p + K_i\frac{1}{s})(p_c - p_c^{ref})}^{\text{PI}} \cdot \overbrace{sat(0,1) \cdot \frac{1}{T_c s + 1}}^{\text{Opening and rate limit}} \cdot(\text{anti-windup})$

Mud Pump Controller	$q_p = q_p^{ref} - q_{d,p_{dh}} - q_{d,\lambda}$ $q_{d,p_{dh}} = \left(\frac{s}{s+1} p_{dh} \overbrace{f_{d,p_{dh}}(u)}^{\text{deadband}} - (sp_{dh})^{ref} \right) K_{p,p_{dh}}$ $q_{d,\lambda} = \left(\frac{s}{s+1} s\lambda f_{d,\lambda}(u) - (s^2\lambda)^{ref} \right) K_{p,\lambda}$
Back Pressure Pump	$q_{d,bpp} = (p_{dh}^{ref} - p_{dh})K_{p,bpp} sat(q_{bpp_{low}}, q_{bpp_{high}})$
Downhole Pressure	$p_{dh} = p_c + \Delta p_{f,a}(q_b, L_a) + \rho_m g h_a$ $p_{dh}^{ref} = p_c^{ref} + \rho_m g L_a * G_{bpp}(q_p^{ref})$ $G_{bpp}(q_p^{ref}) = \begin{cases} 60 & , \quad \text{for } q_p^{ref} = 0 \\ 0 & , \quad \text{else} \end{cases}$
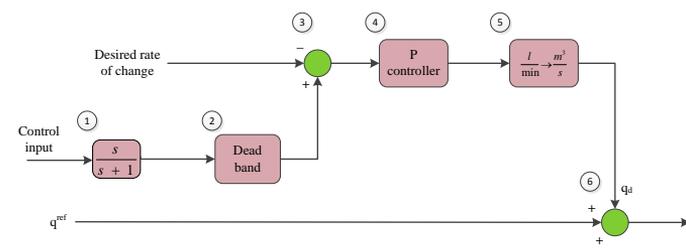
Table 3.2: Overview of the extended MPD system. Constants can be found in App. A

4 | Implementations

This section shows how the MPD system is implemented in Simulink. The characterisics of the components, like the mup pump, choke valve and drilling mud, are shown as well.
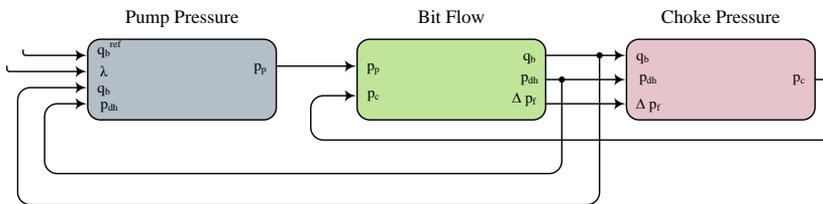

Figure 4.1: A simple overview of the system block diagram, more details are presented in Figure 4.2 on next page.

The MPD system is implemented as three main subsystems as demonstrated in Figure 4.1. In order to easier understand how the different parts of the system are connected, a block representation of the system is provided in Figure 4.2 on the next page. The figure is inteded to resemble a drilling device as well as extending the the simple overview above.
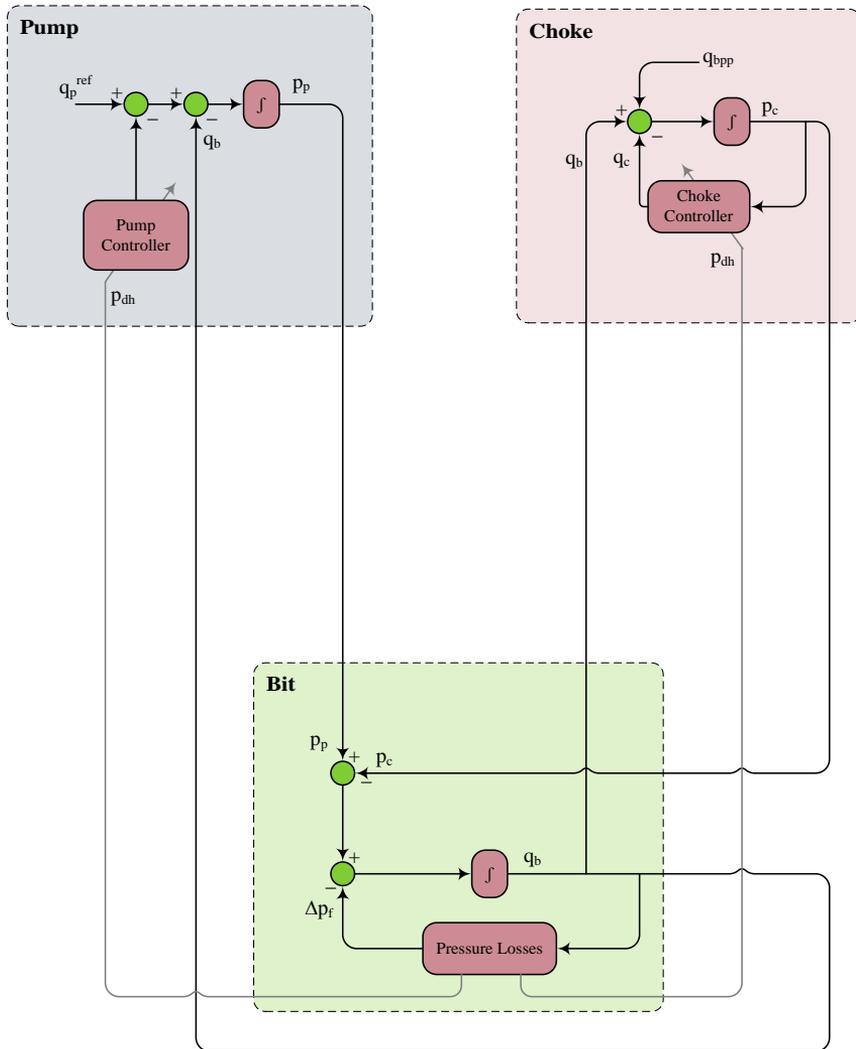
Figure 4.2: An overview of the system, showing how the pump, bit and the choke are connected.

4.1 Implementing the Mud Pump

Input   - Reference flow, q_p^{ref}
             - Bit flow, q_b
             - Downhole pressure, p_{dh}
             - Estimated mud structure, λ

Output   - Pump pressure, p_p

The mud pump is implemented with a step response as a reference flow, q_p^{ref}.
Each of the controllers implemented contains a collection of the blocks called
'Transfer Fcn', 'Dead Zone', 'PID Controller' and 'Saturation'.

The influence from each of the controllers is plotted along with the reference
flow in Figure 4.4. From this simulation there should be noted that the effect
from the controller monitoring the mud structure is quite dominant, compared
to the controller monitoring the downhole pressure. There are two reasons
for implementing it this way. First, when the rate of change of the downhole
pressure increases, there is too late to decrease the flow from the mud pump.
Second, the signal variations are amplified by approximately 500, which is a
lot, making even small changes very exposed. By emphasizing the estimate of
the mud strucure, there is possible to predict pressure variations, and thereby
compesate for that before it happens. All implementations requires a reasonable
estimate of the mud structure.

As a result of including two controllers, the pump flow rate is increased
somewhat slowlier compared to the reference rate, as shown in the lower plot of
Figure 4.4. A closeup of the increase at 25 mins are shown below:
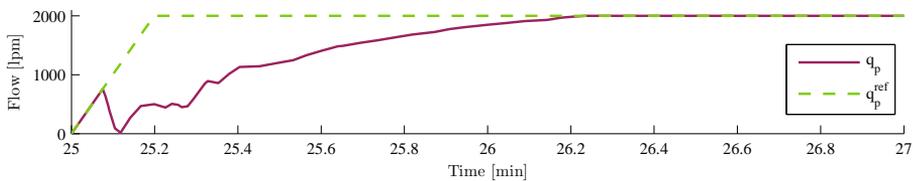
**Figure 4.3:** Figure showing a closeup on 25 min from Figure 4.4.
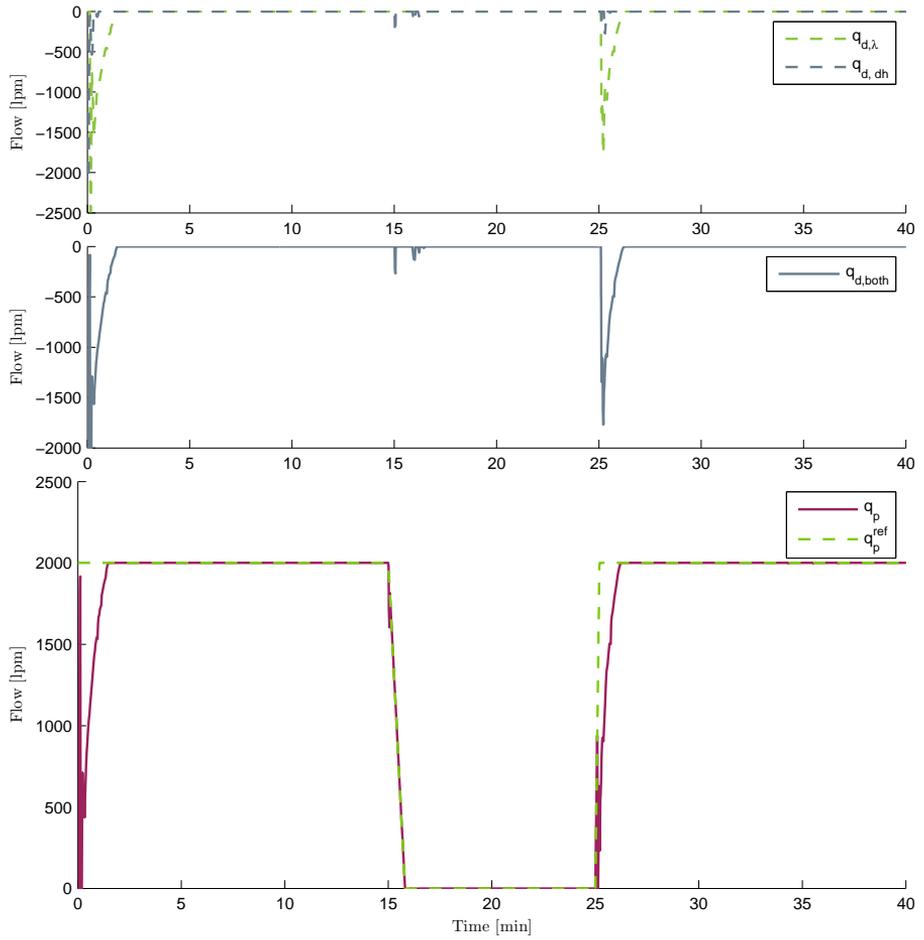
Figure 4.4: An illustration showing how the mud pump works.

4.2 Implementing the Valves

4.2.1 The Check Valve

The check valve is implemented using a 'Max' block in Simulink, adjusted such that no negative flow is allowed. Figure 4.5 presents how the check valve operates. When the pressure outside the bit is sufficiently high, in this case approximately 200 bar, the check valve closes and no flow is allowed backwards in the pipe.
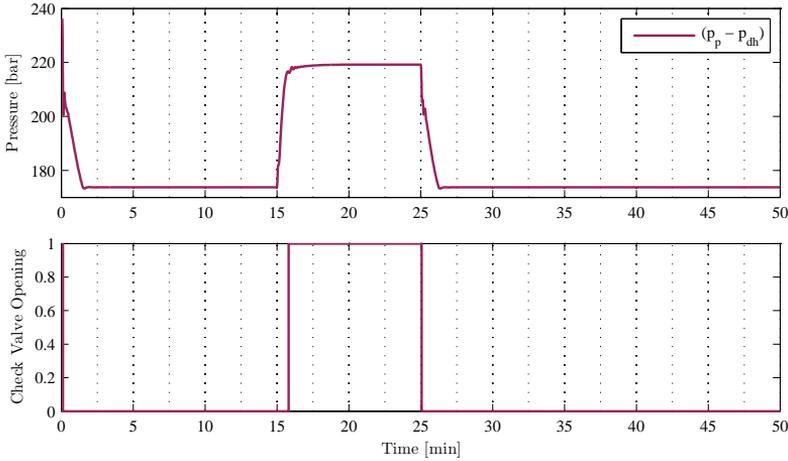

Figure 4.5: An illustration of how the check valve works.

4.2.2 The Choke Valve

The choke valve is implemented according to Eq. (3.34) and (3.35).

$$q_c = kC_v\sqrt{\frac{p_c - p_s}{\rho_m}}g(u) \quad , \quad g(u) = K_p e(t) + K_i e(t)\frac{1}{s}$$

The anti-windup and opening rate limiter is implemented as in Figure 2.9,

where the rate limiter is a transfer function:

$$H(s) = \frac{s}{s+1} \tag{4.1}$$

The choke opening range is limited, meaning that the choke only operate with an opening between 0 and 1.

Valve characteristics

The flow characteristics for the choke valve used in this project are plotted in Figure 4.7, while a sheme for general characteristics are provided in Figure 4.6. The dynamics of the whole system are taken into account, including friction models and fluid viscosity, which may imply that the following comparison is not completly valid. The graph shows similar characteristics as for the 'linear percentage line' in Figure 4.6. Some nonlinearities are observed around $q_c = 500$, which might be due to the non-linear friction in the system (described in Section 2.2.2).
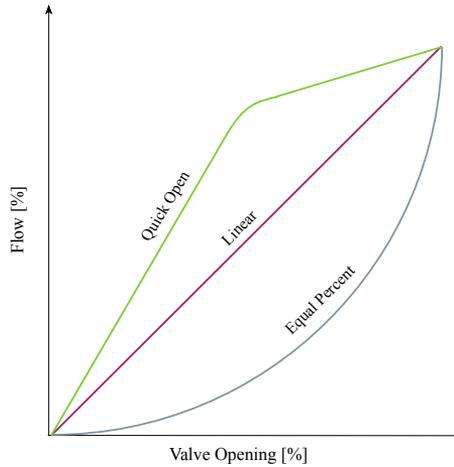

**Figure 4.6:** A revisit of the figure from the theory.
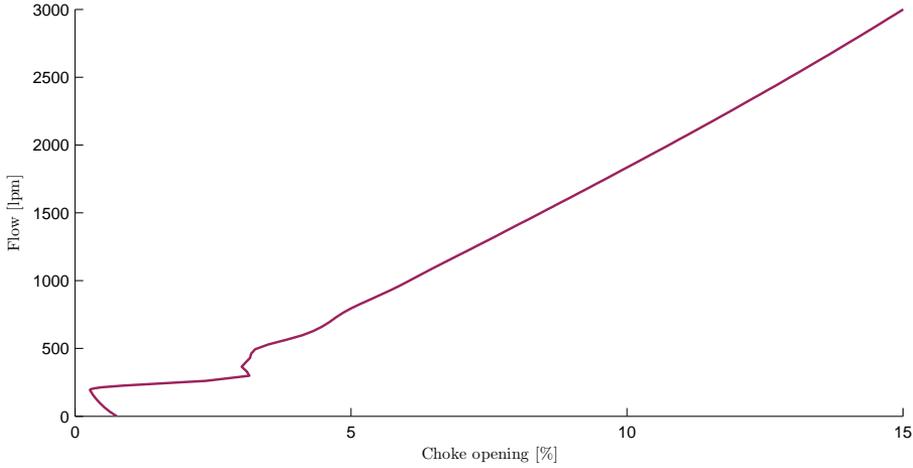
Figure 4.7: Choke charateristics; the pump flow is ramped up from 0 lpm to 3000 lpm.

4.3 Implementing the Back Pressure Pump

4.3.1 Constant Flow

The back pressure pump is set to motion when $q_p^{ref} = 0$. This is done by first using identical step times for both the mud pump and the back pressure pump. The signal is thereafter amplified, converted to $\frac{m^3}{s}$ and finally added as a disturbance to the choke flow.
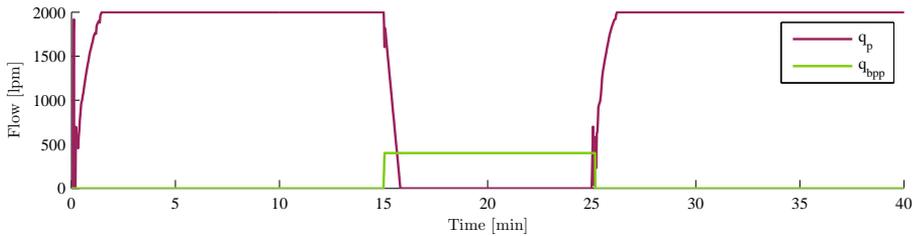

Figure 4.8: Back pressure pump implemented as a constant flow rate.

4.3.2   Controlled Flow

The result of the implementation of an automated back pressured pump, according to Eq. (3.43) are presented below.
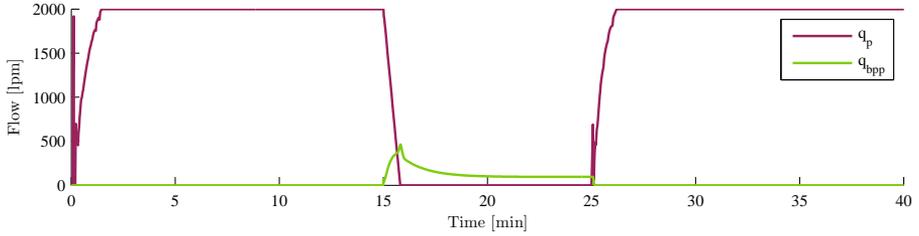

Figure 4.9: The Automated Back pressure pump.

4.4   Implementation of the Drilling Mud

The mud properties are implemented by the friction models described in previous chapters (see summaries in Table 3.1 and 3.2). Approximately 70% of the frictional pressure loss occurs in the annulus, while the remaining 30% occurs in the drillstring and the bit. Figure 4.10a demonstrates how the pressure drops due to friction, while Figure 4.10b presents the mud structure changes with respect to flow rate and time. The thixotropic behavour of the mud is apparent as the nonlinar decreases when the flow rate is constant (the input flow is the same as in Figure 4.4). Because of the additional time-dependent friction term in the Cheng model, the pressure drop will never reach zero, as seen below.

As mentioned in the theory, there was expected to see a tendency of hysteresis during simulation. Figure 4.11 includes the pressure drop for increasing and decreasing flow. As expected, the pressure loss is significantly lower for decreasing flow, because the mud is already liquid. A comparison to the expected result is presented in Figure 4.12. The trend is similar, higher and lower pressure loss due to increasing and decreasing flow rate, respectively. Moreover, an oscillating trend for the purple line is assumed to be a result of the gel-breaking process.

54

(a) Pressure loss due to friction, Δp_f.

(b) Mud structure parameter, λ.

**Figure 4.10:** Figure showing the properties of the drilling mud.
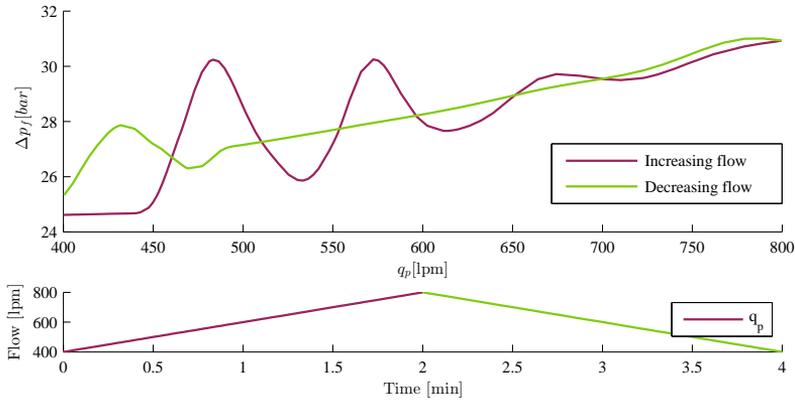
Figure 4.11: Figure showing the properties of hysterese for the drilling mud.

55
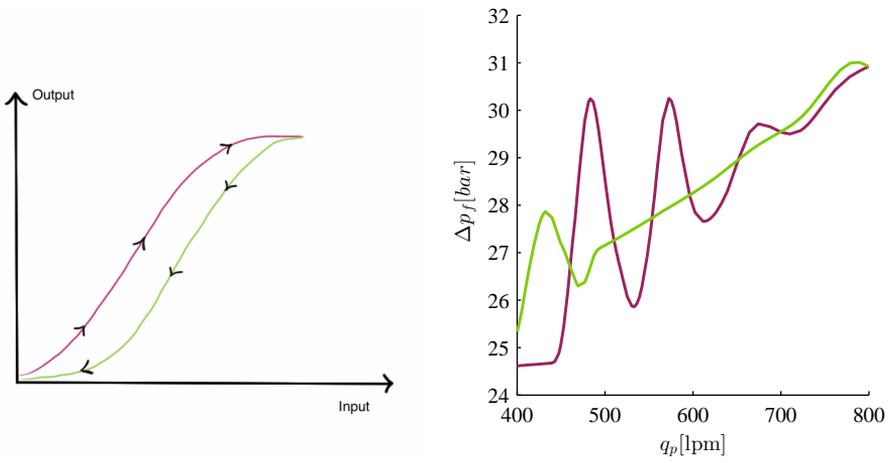
(a) Theoretical hysteresis

(b) Simulated hysteresis

Figure 4.12: Figure showing the hysteresis from the theory compared to the simulated hysteresis in Figure 4.11

5 | Results and Discussion

This chapter will, for the reader's convenience, provide the resulting plots as well as related discussion. There are two main sections, one describing a regular MPD scenario, the other testing the robustness of the system.

5.1 Downhole Pressure Control

In a regular MDP scenario the mud pump is shut down for approximately 10 minutes and then restarted. The 40-minute simulation includes, in this project, two start-ups, one from a fully gelled structure ($\lambda \simeq 0.8$) and one where the mud is in the process of gelling.

5.1.1 Standard vs. Extended MPD

The difference between the standard and the extended MPD system is demonstrated in Figure 5.1. The purpose of including an automated mud pump was to keep the pressure variations within the limits of $\pm$ 2 bar (the gray lines). The following observations are noteworthy:

- *0 - 2 min:* Starting the mud pump when the mud is fully gelled caused a pressure peak of approximately 10 bars without the automated mud pump. Including the controller results in a small pressure peak of 2 bar. Yet, the pressure does not exceed the reference pressure and is therefore assumed to be of no concern.

- *25 - 27 min*: The standard MPD system shows a significantly large peak when starting up the pump after a break, while the extended MPD system remains within the ± 2 bar limit lines. The drop below 245 bar is caused by the back pressure pump being shut down too rapidly.

Practical Aspects

One of the purposes of an automated mud pump was to attain a system that quickly returned to drilling after a shutdown, without pushing the gelled excessively. The effect of the controller was a decreased flow rate whenever the pressure increased at an excessive rate, leading to more acceptable pressure variations, as demonstrated in Figure 5.1c. Saving several seconds every time the mud pump is started, which is rather frequently during a day, can result in significant cost reduction.

It is current industrial practice to ramp up the mud pump manually. However, an automated mud pump can result in the need for fewer workers, meaning lower payroll cost. Moreover, the workers on site have long workdays and there is a real risk of making mistakes. Using measurements and calculations from a computer might therefore lead to less risk of failures, assuming the calculations are reliable.

In order to trust the automated mud pump, there must be a guarantee that there is a pendable mud structure model. The downhole pressure calculations also need to be credible. However, direct measurement from the drill bit nowadays is not reliable (Imsland; n.d.), therefore, a choke measurement is utilized to calculate the downhole pressure.

5.1.2 Pump Control vs Choke Control

The influence from each of the controlled components, the choke valve and the mud pump respectively, are shown in Figure 5.2. It can be observed that the choke valve (blue line) works well without the automated pump. Still, the large pressure peaks mentioned earlier are apparent.

On the other hand, the pump controller does not work properly without
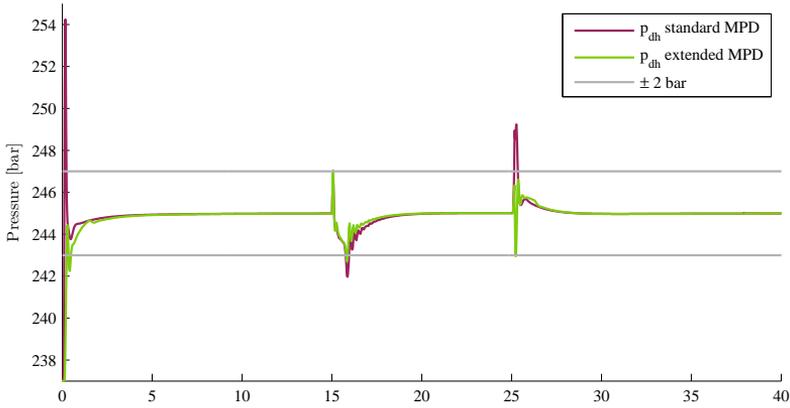
(a) Downhole pressure shown for both the standard and the extended MPD system.
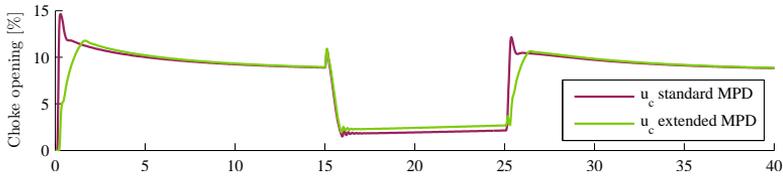
(b) Plot showing how the choke valve is working in each case.
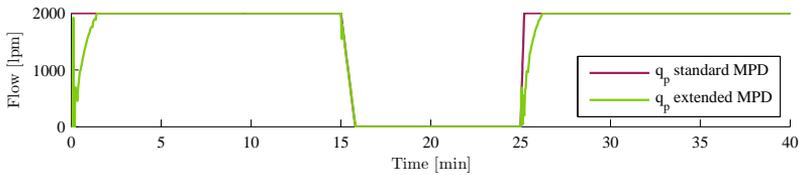
(c) Plot showing the flow provided by the mud pump.

Figure 5.1: The downhole pressure before and after inserting a controller for the mud pump (back pressure pump is not plotted). The gray lines shows the limits of where the downhole pressure should remain.

the choke valve, which is expected since it is not meant for a system without a choke. It does, in fact, suppress the small bumps (lowest dashed line), but there is no chance it can reach reference pressure. If so, the pipes must be of much smaller dimensions, probably around the same dimensions corresponding to a choke opening of 15%.

As a result, the pump controller requires a reasonable tuned choke valve, as well as a timely back pressure pump in order to maintain a stable downhole pressure.
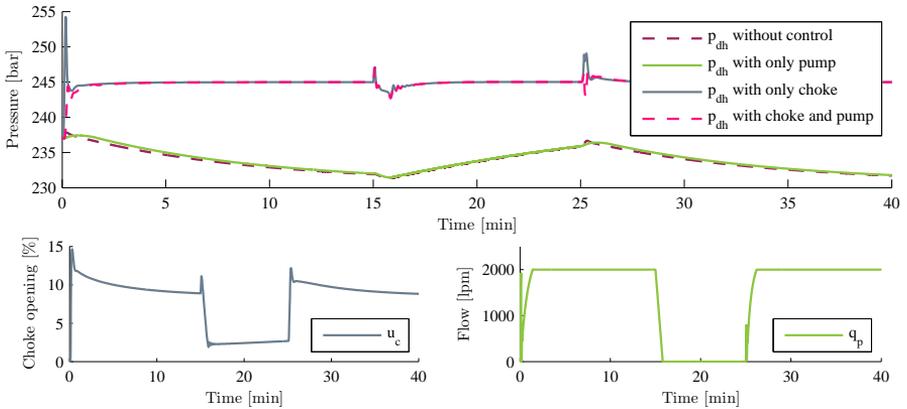

Figure 5.2: Figure showing the influence from each of the controllers.

5.1.3   The Mud Pump Controllers

As mentioned in the theory in Section 3.2.1, the automated mud pump includes two controllers. The influence from these two controllers, along with two close-ups of the response subsequent startup are demonstrated in Figure 5.3.

When focusing on the closup in Figure 5.3b, where the mud is fully gelled, four graphs are present. Without any pump control, the overshoot is approximately 10 bars, which is excessive. Using only the downhole pressure as a control input, the overshoot is decreased by 3 bar, which still exceeds the $\pm$ 2 bar range. On the other hand, an overshoot of a bit more than a bar can be seen when the estimated mud structure is used as the only input. However, using

both, the overshoot can hardly be called a peak anymore and is represented by the dashed pink line.

Another aspect to have in mind is *the amount of time* the mud pump requires in order to return to the reference flow. This is covered more closely in Section 5.2.2.
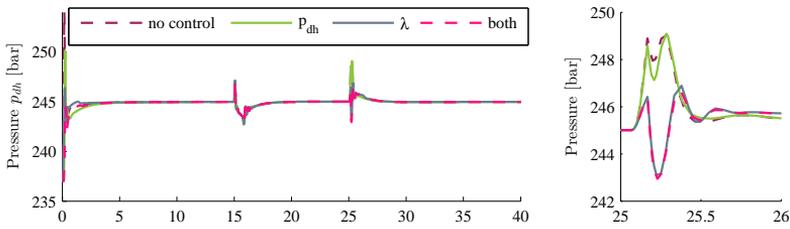
(a) Overview, showing the whole shut down and start up as well as a closer look at the startup after a short break.
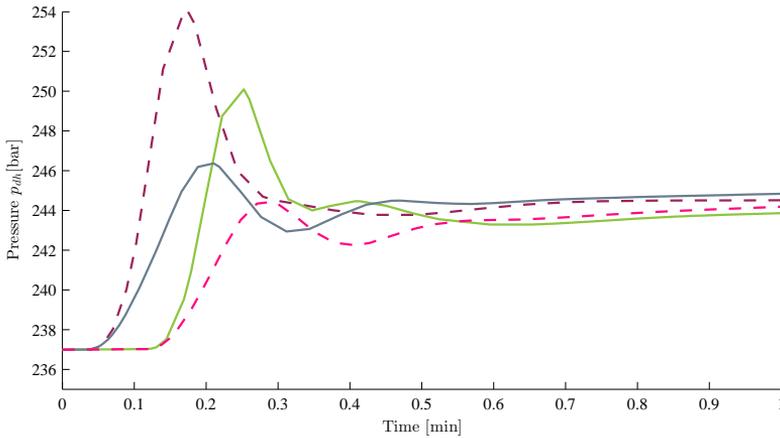
(b) A closer look at the start up after fully gelled mud. Legends as in a).

Figure 5.3: Figure showing the influence from each of the pump controllers.

5.1.4 An Automated Back Pressure Pump

As mentioned in Section 3.2.2, there might be possible to incorporate automatic control to the back pressure pump. Normally, the back pressure pump is just a constant flow which starts whenever the mud pump is shut down. Having only a constant flow, however, can make it problematic to obtain precise start-up and shutdown timing, which was one of the reasons for the additional pressure peaks in Figure 5.1 on page 59. For this reason, a P controller according to Eq. (3.43) on page 43 was added and is presented in Figure 5.4, with the result that these peaks are no longer apparent. This might be an advantage if unplanned shutdown of the mud pump should occur.

Comparing the green and purple line in the upper plot of Figure 5.4, improvements in the downhole pressure are observed when the backpressure pump is automated. That is, the peaks are approximately one bar smaller and there is significantly less variation in the pressure (the green line, in contrast, looks noisy). Even though an automated back pressure pump provided a higher flow rate to the system compared to the constant flow, an increased flow rate did not provide any improvements.
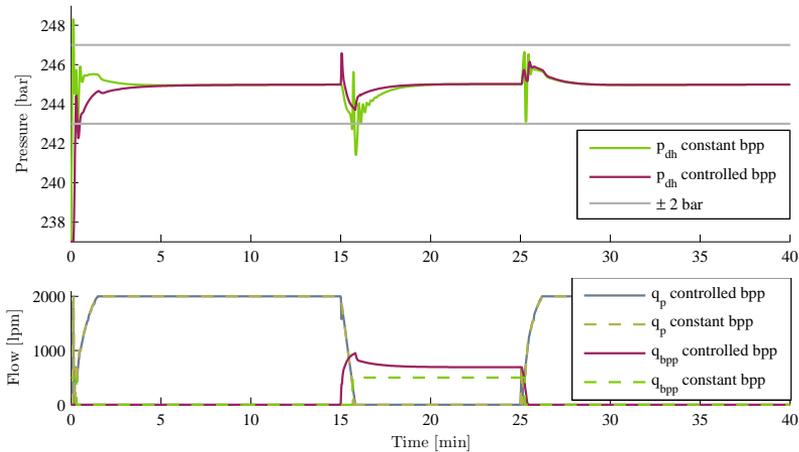

Figure 5.4: Figure showing the back pressure pump with and without controller

As previously mentioned, the controlled back pressure pump led to less variations in the downhole pressure, which might be an advantage when it comes to dowhole equipment wear. The graphs in Figure 5.5 show how the choke valve responds to the two scenarios. It is observed that the pressure variations caused by the uncontrolled flow rate affects the choke valve opening. The blue line, however, shows a considerably smoother control of the choke valve, which might lead to less wear and tear.
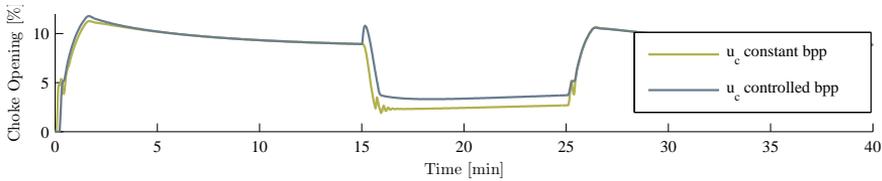

Figure 5.5: Choke valve opening with constant and controlled back pressure pump.

Practical aspects

An automated back pressure pump might offer several advantages. It frees the valve from overall pressure control and can further stabilize the downhole pressure by providing a more precise startup and shutdown.

With this is mind, using a controller on the back pressure pump has to be less expensive as against the cost of wear on the choke valve. In addition, the back pressure pump will only affect the downhole pressure during the shutdown of the mud pump, after which the mud will be gelled.

5.2 The Robustness of the System

The previous section focused on a standard scenario where the pump was started up, shut down, and then started up again. Other test scenarios may be convenient to further investigate the properties and the robustness of the system. This

section will therefore discuss the tests of the system for different flow rates as well as varoius shutdown periods.

5.2.1 Stepping up

The graphs to the right presents the system responds to varoius of input flows. First, the mud pump reference is ramped up 1000 lpm every 400 sec (approx. 6 mins). Then, the pump is gradually ramped down to zero again as shown in Figure 5.6. Every time q_p is below 500 lpm, the constant back pressure pump will start.

By looking at Figure 5.6b, it can be seen that the downhole pressure is well within the ± 2 bar limits for flow between 1000 and 3000 lpm. Even though the mud becomes more fluent for every flow step, the downhole pressure peaks are of approximately equal heigth. Some of the thixotropic effect can neverhteless be seen in Figure 5.6a as a nonlinear respons from the choke. The effect is more appearent for increased flow compared to decreased flow, which is natural because this is where the gelling occurs.

5.2.2 Shutting down for a longer period

When drilling, the mud pump may be shut down for a varoius amount of time. Figure 5.7 demonstrate what occurs to the downhole pressure when the pump is shut down for 5, 10 and 18 minutes.

The green, purple and blue lines in the lower subplot Figure 5.7 represent the short, medium and long shut down time, respectively. These shutdown times affect the dowhole pressure according to the correspoding upper graph. As can be seen, the difference of the peak heights are not substantial, but as the amount of down-time for the mud pump increases, the peaks is actually smaller. This tendency can be seen even though the mud has more time to gel, illustrated in Figure 5.8 below:

64

(a) The two control parts, input flow (green) and choke opening.

(b) The resulting downhole pressure due to increased and decreased input flow.
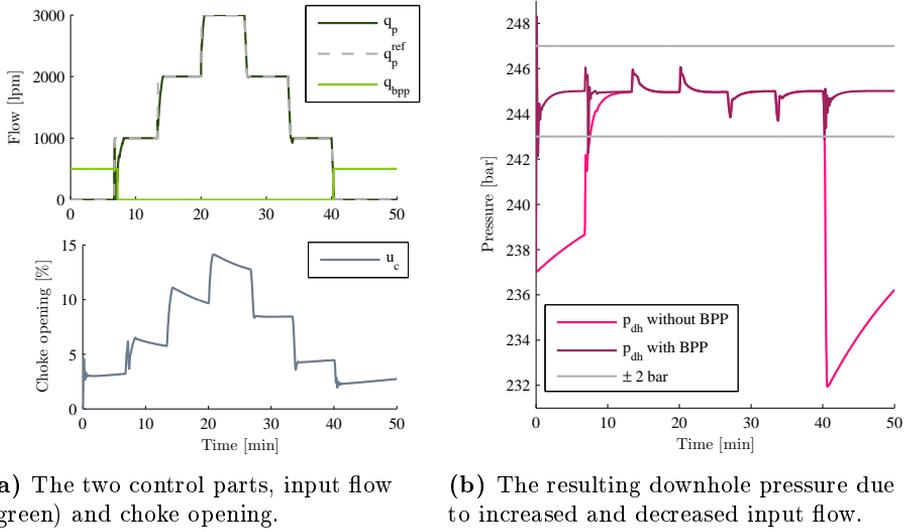
Figure 5.6: A figure showing how the downhole pressure changes when the mud pump is stepped up and down.
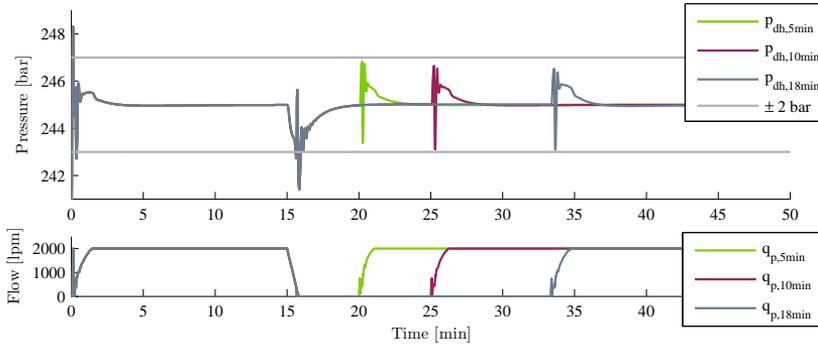

Figure 5.7: Figure showing how downhole pressure reacts on different shut down times.
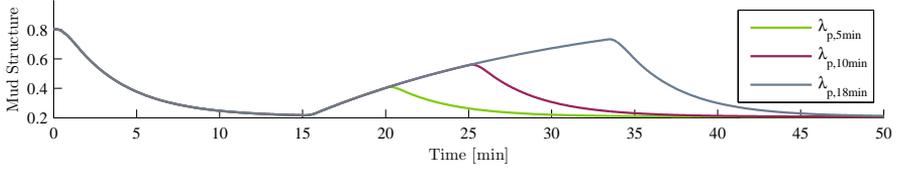
Figure 5.8: The figure shows how the mud structure increases according to the mud pump shut downs in Figure 5.7 above.
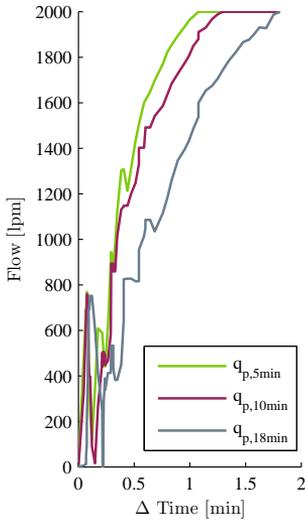
Figure 5.9: Closeup from 5.7, showing how much time the mup pump ramp time.

During the longest idle period (18 minutes) the mud becomes almost fully gelled, as $\lambda \simeq 0.8$. Still the controller manage to keep the downhole pressure below the limit quite well.

The flow rates in the lower plot of Figure 5.7 seems to have an identical flow rate trend when returning to 2000 lpm. Because of the time range, the amout of time spent to reach 2000 lpm looks similar. Nonetheless, a closeup is provided in Figure 5.9 to the left, where the three ramps from Figure 5.7 is plotted on top of eachother to better display the differences. As can be seen, the longer the mup pumps has been shut down, the longer time it takes to reach 2000 lpm.

6 | Conclusion and Further Work

6.1 Conclusion

The purpose of this project was to maintain a constant downhole pressure during the fastest possible startup procedure. In order to achieve this goal, controllers were added to both the mud pump and the back pressure pump, where the main focus was on the mud pump.

When incorporating automatic control to the mud pump, it was found that the downhole pressure could be kept within the $\pm$ 2 bar boundaries. This was because the controller slowed down the pump flow whenever the pressure increased too fast. The mud pump controller also relieved the choke valve from the overall pressure control, leading to less need of alterations for the choke valve opening. Such oscillations might cause damage and unnecessary wear and tear.

The mud pump controller consisted of two controllers, one monitoring the downhole pressure and one using an estimation of the mud structure, λ, as an input. Using both the downhole pressure and λ resulted in a reasonable approach to an optimal flow increase, assuming that λ could be correctly calculated and that pressure measurement from down hole are avaiable.

Due to the problems that arose when timing the back pressure pump, as well as the oscillations in the choke valve, a controller was added to the back pressure pump. This resulted in more precise startup of the pump, such that no considerable pressure peaks could be observed when the mud pump was shut

down. The choke valve oscillations were also eliminated.

Even though both the downhole pressure control and the choke valve stabilization were improved using a controller on the back pressure pump, the system works adequately without one. The main difference is after all only a matter of seconds when the mud pump shuts down and the backpressure pump is turned on. Whether there is a point of implementing a controller, would depend on the particular requirements of the system.

Having three controllers in the system, care must be taken that they do not work against each other. The choke valve controller is the only controller having a PI-controller, while the two others use a P controller because several integral controllers might cause heavy windup.

6.2   Further Work

The two controllers added to the mud pump and the back pressure pump are simple P controllers. Integral action might improve the control effect, but as mentioned above, care must be taken in order to prevent unwanted effects. Using a controller on the back pressure pump should be reconsidered in terms of what the drilling industry actually needs.

Gelling was implemented using the Cheng model, which might not be an optimal model of the mud. Other friction models can be found by looking at work done for the cement industry, and, believe it or not, the yoghurt industry. These industries use thixotropic models when describing their fluids, where gelling, or hardening, is of high importance. Another aspect to consider is the gel breaking. In this project no rotation of the drillstring was included, and neither were temperature changes. Lubrications close to the drillstring will occur and unequal sized cutting particles might have a heavy impact on the gel breaking procedure.

A |

Constants

Where	Constant	Unit
Basic Model	$\beta_d = 15000$	bar
	$\beta_a = 15000$	bar
	$M_d = 6000$	bar $\cdot s^2 \cdot m^2$
	$M_a = 1600$	bar $\cdot s^2 \cdot m^2$
	$p_c^{ref} = 14.1$	bar
	$p_{dh}^{ref} = 245$	bar
	$p_{p,ss} = 188.8$	bar
	$q_{b,ss} = 2000$	lpm
	$T_c = 18.9$	sec
	$T_{windup} = 0.1$	sec
	$K_p = 0.05$	
	$K_i = 0.0008$	
	$k = 0.0865$	

	$C_v = 41$	USG$/($min$\cdot\sqrt{\psi})$
	$C_b = 0.98$	
	$C_{sc} = 0.5$	
	$A = \frac{\pi}{4}\frac{(15^2+15^2+16^2+16^2)}{32^2}$	in^2
The Cheng Model	$\tau_0 = 7.5$	Pa
	$\tau_1 = 40.5$	Pa
	$\mu_p = 16 \cdot 10^{-3}$	bar $\cdot$ s
	$\lambda_{init} = 0.8$	
	$a = 1 \cdot 10^{-3}$	$\frac{1}{s}$
	$b = 1.44 \cdot 10^{-5}$	
Geometry	$L_d = 4019$	m
	$L_a = 4000$	m
	$h_a = 1826$	m
	$d_i = 0.1086$	m
	$d_o = 0.1270$	m
	$d_h = 0.2454$	m
	$A_a = \pi(d_h - d_o)$	m^2
	$V_d = \frac{\pi}{4}d_i^2 L_d$	m^3
	$V_a = \frac{\pi}{4}(d_h^2 - d_o^2)L_a$	m^3
Rheology	$\rho_{H_2O} = 1000$	kg$/m^3$
	$g = 9.81$	m$/s^2$
	$g_s = 1.18$	m$/s^2$
	$p_s = 1$	bar
Controllers	$K_p = 0.05$	
	$K_i = 0.0008$	
	$T_c = 18.9$	
	$K_{p,p_{dh}} = 500$	
	$K_{p,\lambda} = 25 \cdot 10^6$	
	$K_{p,bpp} = 200$	

Table A.1: All the constants used in the thesis

B |

Variables

	Variable	Range	Unit
Basic Model	p_p	$[0, 80]$	bar
	p_c	$[0, 16]$	bar
	q_b	$[0, 3000]$	lpm
	q_p	$[0, 3000]$	lpm
	q_c	$[0, 3000]$	lpm
	$q_{d,bpp}$	$[-700, 0]$	lpm
The Cheng Model	λ	$[0, 1]$	
Extended Model	$q_{d,p_{dh}}$	$[-2000, 0]$	lpm
	$q_{d,\lambda}$	$[-2000, 0]$	lpm

Table B.1: Variables used in the various models, including their range and limits.

APPENDIX B.
VARIABLES

D

C

Software

 TexStudio

 Visio

 Sketchbook Pro

 mindjet

APPENDIX C.
SOFTWARE

F

Bibliography

Barnes, H. A. (1997). Thixotrophy - a review.

Bemporad, P. A. (2010). Anti-windup techniques.

Bengt Aberg, S. A. (1997). Drill bit having springless check valve and method of blocking backflow during drilling, `http://www.google.it/patents/US5645132`. Accessed February 27, 2014.

Bremer, J. (2008). Pipeline flow of settling slurries, `https://www.engineersaustralia.org.au/sites/default/files/shado/Learned%20Groups/Colleges/Mechanical%20College/WA%20Branch/Pipeline%20Transport%20of%20Settling%20Slurries%20(Presentation%20without%20Audio).pdf`. Accessed March 11, 2014.

Daniel A. Vallero, T. M. L. (2013). Unraveling Environmental Disasters.

Glenn-Ole Kaasa, Oyvind Nilstad Stamnes, Lars Imsland, Ole Morten Aamo (2012). Simplified Hydraulics Model Used for Intelligent Estimation of Downhole Pressure for a Managed-Pressure-Drilling Control System.

Hubbard, A. T. (2002). Encyclopedia of Surface and Colloid Science , Volume 1.

Imsland, L. (2008). Model of drilling hydraulics for adaptive pressure estimation.

Imsland, L. (n.d.). Supervisor.

BIBLIOGRAPHY

J. Sestak, M. Houska, R. Z. (1982). Mixing of Thixotropic Fluids.

Kittelsen, P. (n.d.). Madi sop dpo.

Landet, I. S. (2010). Modeling and Control for Managed Pressure Drilling from Floaters.

Management, E. P. (2005). Control Valve Handbook.
    URL: *http://www.documentation.emersonprocess.com/groups/public/documents/book/cvh9*

MiSwaco (2013). Drilling chokes - ultimate pressure control for the most challenging applications, `http://www.slb.com/~/media/Files/miswaco/brochures/Drilling_Chokes.pdf`.

Olav Egeland, J. T. G. (2002). Modelling and Simulation for Automatic Control.

Rasmus, J. (2013). Methods for evaluating borehole volume changes while drilling, `http://www.faqs.org/patents/app/20130090854`. Accessed February 27, 2014.

Swensen, I. (2013). Modelling and non-linear control of gel breaking in drilling operations.

tyco Water (n.d.). Gate valves (for australian waterworks), `http://water.pentair.com/water/Images/TDS-Gate-Valve-Range-Overview.pdf`. Accessed February 27, 2014.

UIPAC (2011). Terminology of polymers and polymerization processes in dispersed systems (IUPAC Recommendations 2011).

Valve (n.d.). `http://en.wikipedia.org/wiki/Valve`. Accessed February 27, 2014.

Welander, P. (2010). Understanding derivative in pid control, `http://www.controleng.com/search/search-single-display/understanding-derivative-in-pid-control/4ea87c406e.html`. Accessed February 6, 2014.

White, F. M. (2008). Fluid Mechanics, 6th Edition.

H